ABSTRACT

Title of Document:	SCINTILLATION CONDITIONING OF TANTALUM CAPACITORS WITH MANGANESE DIOXIDE CATHODES Thomas Fritzler, Master of Science, 2013
Directed By:	Professor Michael G. Pecht, Mechanical Engineering Assistant Research Scientist Michael H. Azarian, Mechanical Engineering

Scintillation testing is a method that activates the self-healing mechanism in tantalum capacitors. In preliminary experiments, the deliberate activation of self-healing yielded up to 27% higher breakdown voltages in weak parts that had an increased risk of ignition failure. This improvement results in a better performance under surge current conditions. This paper demonstrates that scintillation conditioning reduces surge current failures in tantalum capacitors with manganese dioxide cathodes. Tantalum capacitors with MnO_2 cathodes from two manufacturers are subjected to scintillation conditioning and compared to non-conditioned populations in a surge current test. To ensure that the activation of the self-healing mechanism has no detrimental effect on the reliability of the parts, a life test is conducted. The results show that the conditioning method increases the breakdown voltage of self-healed tantalum capacitors by up to 25% under surge current conditions, which mitigates the risk of ignition failures. No detrimental effect on the life of the conditioned samples was observed.

Additional tests to assess the reliability of tantalum capacitors with manganese dioxide cathodes under simultaneous thermo-mechanical and voltage stresses were performed. Even though these tests are not directly related to scintillation conditioning the study was included as an additional chapter, since it pertains to the general subject of tantalum capacitor reliability.

SCINTILLATION CONDITIONING OF TANTALUM CAPACITORS WITH MANGANESE DIOXIDE CATHODES

By

Thomas Fritzler

Thesis submitted to the Faculty of the Graduate School of the
University of Maryland, College Park, in partial fulfillment
of the requirements for the degree of
Master of Science
2013

Advisory Committee:
Professor Michael G. Pecht, Chair
Professor Patrick McCluskey
Assistant Research Scientist Michael H. Azarian

DEDICATION

To my parents and my brother Alex.

ACKNOWLEDGEMENTS

I would like to thank Dr. Azarian for his help and guidance throughout the graduate program and thesis. Without his support and the discussions that yielded in constructive suggestions and criticism I would not have been able to accomplish the thesis. I also thank Prof. Pecht for the opportunity to pursue a graduate degree as well as the time, patience, and guidance provided in this effort. I thank the faculty of the CALCE, Electronics Product and Systems, especially Bhanu and Swapnesh, for their technical support and expertise that contributed to my thesis. I would like to thank Hannes as well, for the patience and countless suggestions for improvements.

I also wish to thank Prof. McCluskey for being on my thesis committee and his valuable comments that help me in improving my work.

Finally, I thank my parents and brother who respected and supported my decision to pursue a graduate degree in a foreign country. Lending a listening ear to me during the stressful times was what kept me going to the end.

TABLE OF CONTENTS

LIST OF TABLES

LIST OF FIGURES

1 CHAPTER 1: SCINTILLATION CONDITIONING OF TANTALUM CAPACITORS WITH MANGANESE DIOXIDE CATHODES

1.1 INTRODUCTION

The advantages of tantalum capacitors with manganese dioxide cathodes are high volumetric efficiencies of more than 100,000 CV/g (Capacitance x voltage/gram) [1], stability of their capacitance over their rated temperature range within 5% [2], and the ability to self-heal after dielectric breakdown [3]–[5]. However, the application range of tantalum capacitors is limited due to the low maximum rated voltage of 50V of currently existing capacitor designs. Dielectric breakdown of tantalum capacitors with manganese dioxide can be problematic under large surge currents, since the parts can ignite and damage surrounding components and circuitry. Manufacturing defects and impurities can cause surge current failures due to a reduction of the breakdown voltage [6], [7]. In addition, thermo-mechanical stresses experienced during the reflow process can exacerbate the failure rate [8]–[10]. Since tantalum capacitors are increasingly used in low impedance applications due to their long life, volumetric efficiency, small size, and the development of tantalum capacitors with even higher CV products, the potential damage due to surge current failures is expected to increase [6].

Despite the employment of screening methods suggested to “ensure” that tantalum capacitors are capable of withstanding surge currents in their application conditions [11], [12], failures during the power-on process of surge current screened tantalum capacitors have been reported [8]–[10]. The failure voltages were found to be in some cases even lower than the rated voltage [8]–[10]. The risk of ignition failure is further increased if voltage transients occur when switching on the power supply. Surge current failures occur due to impurities within the dielectric and dielectric thickness variations that reduce the breakdown voltage [6], [7]. Our preliminary research, as well as other research [6]–[9], suggested that the self-healing mechanism of tantalum capacitors has the potential to isolate these defects as well as defects created by thermo-mechanical stresses during the reflow process, which could result in surge current failures. Therefore, a conditioning method based on scintillation testing was developed that either screened out samples that were not capable of withstanding a predetermined voltage or conditioned weak samples by activating the self-healing mechanism to improve their breakdown voltage. The improvement was expected to minimize failures under surge current conditions. Since the self-healing mechanism initiated a conversion of materials within the capacitors, a life test was conducted to exclude the possibility that the life of the parts was degraded or that new failure mechanisms were introduced due to the conditioning method.

1.1.1 SOLID TANTALUM CAPACITOR MANUFACTURING PROCESS AND CONSTRUCTION

While there are different mounting technologies of solid tantalum capacitors such as lead frames and end terminations, this study was focused on tantalum capacitors with lead frames as illustrated in Figure 1.

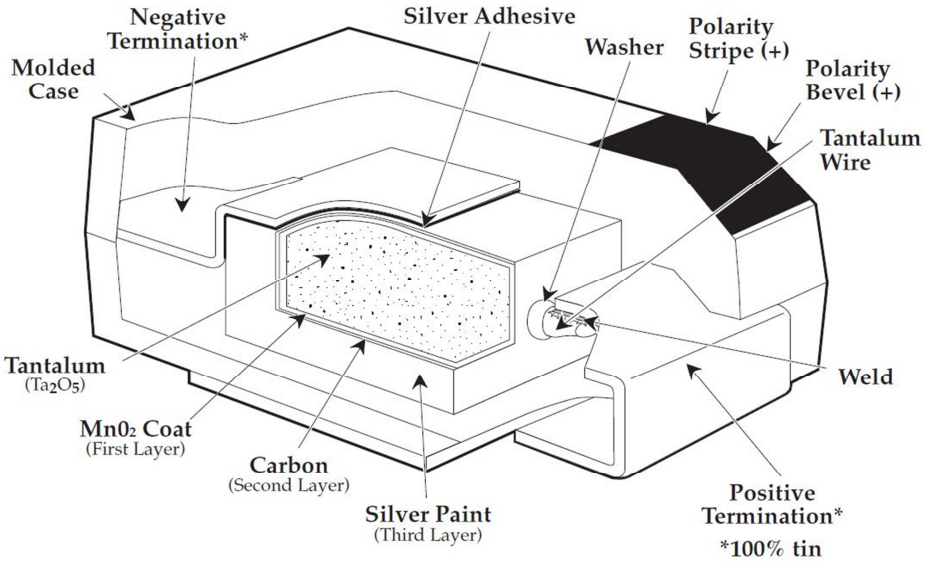

Figure 1: Schematic of tantalum capacitor with manganese dioxide cathode construction [13].

Tantalum capacitors are manufactured using pure tantalum metal in powder form. Since the surface area is proportional to the capacitance,

$$C = E_R \cdot E_0 * A/d \qquad (1)$$

C: Capacitance in Farad [F]
E_R: Dielectric constant [-]
E_0: Electric constant [Fm^{-1}]
A: Area of overlap between two opposing plates [m]
D: Separation between two opposing plates [m],

a low tantalum powder particle size is desired, which results in particle sizes on the micrometer scale [13]. The powder is pressed around a tantalum wire to form the anode. This structure is also commonly referred to as “slug”. In order to fuse the individual particles permanently, the tantalum slug is sintered at high temperatures between 1500°C and 2000°C. This causes the structure not only to gain mechanical strength but also to maintain its porosity, which results in a surface area or capacitance. The next step involves forming the insulation dielectric layer on top of the anode material. The process responsible for the formation of the dielectric layer is anodization, in which the tantalum slug is dipped into an acidic solution while a voltage (formation voltage) is applied. This

forms an amorphous tantalum pentoxide layer (Ta_2O_5), whose thickness can be controlled by variation of the voltage level and the duration of the voltage application. The formation voltage is typically two to three times higher than the parts` rated voltage to guarantee a satisfactory reliability [13]. Impurities in the anode material can have a significant effect on the reliability of the parts, since they affect the leakage and dielectric breakdown behavior depending on their location and distribution in the anode and dielectric.
In the subsequent step the manganese dioxide (MnO_2) cathode layer is formed using pyrolysis. The slug with the formed dielectric layer is dipped into manganese nitrate and baked at about 250°C. The process is repeated multiple times to make sure that the inner surfaces of the porous body are covered by a consistent manganese dioxide layer.
A graphite layer is applied by dipping the part into a graphite solution to avoid a chemical reaction between the manganese dioxide and the silver adhesive layer, which is used to attach the lead frame.
The cathode lead frame is attached using silver loaded epoxy, whereas the tantalum wire is welded to the anode lead frame. In the last step the capacitor structure is embedded in a mold compound.

1.1.2 Failure Mechanisms and Modes of Tantalum Capacitors

Reliability concerns with tantalum capacitors are often associated with the degradation of the dielectric layer Ta_2O_5 (tantalum pentoxide), which can lead to dielectric breakdown. Leakage current is the most sensitive electrical parameter indicating the degradation of the dielectric of tantalum capacitors. Various failure mechanisms are believed to be responsible for the degradation of the dielectric. Failures under steady-state conditions that experience a sharp increase of leakage current can be explained with field crystallization, which usually is observed in areas with high contents of impurities [14]. The dielectric layer Ta_2O_5 is in an inherently thermodynamically unstable state that tends to reduce the high energy level of its amorphous structure through crystallization [15]–[21]. In the process of localized crystallization, the crystallized material changes its density, thus creating stress states in the amorphous matrix that can crack the Ta_2O_5 layer. The crystal growth rate is believed to be a determining factor of the life of tantalum capacitors [14].
Another failure mechanism responsible for failures under steady-state operation is believed to be oxygen migration. Concentrated oxygen in vicinity of the electrodes is responsible for low conductivity of the dielectric [19]. The oxygen gradient between the neighboring layers, tantalum and tantalum pentoxide, causes oxygen migration due to their affinity towards equilibrium between the two layers [15]. As the oxygen migrates towards the tantalum metal, oxygen vacancies are created in the dielectric layer. As the density of oxygen vacancies increases, the leakage current in the capacitor increases [19]. Both failure mechanisms, field crystallization and oxygen migration, are exponentially accelerated by temperature stress [15], whereas crystallization can also be accelerated by

electrical stress [14], [16], [17][14], [16], [17]. The quality and integrity of tantalum capacitors is usually assessed by measuring the leakage current. A gradual increase of leakage current can indicate a wear out mechanism such as field crystallization or oxygen migration.

In the event of overstresses tantalum capacitors can fail in an ignition mode under surge conditions (Figure 2). If the dielectric breakdown voltage is exceeded, breakdown of the dielectric occurs, which forms a localized conductive path. This path of low resistance leads to a current concentration, which can be observed as a sudden increase of leakage current. The locally constricted current increase results in a temperature rise. If the magnitude of current is not restricted and enough current is supplied through the breakdown site, a chain reaction starts at about 480°C that allows Ta_2O_5 to change from an insulating, amorphous state into a conductive, crystalline state [3], [22]. As the crystalline Ta_2O_5 area increases, the current is distributed and converts more amorphous Ta_2O_5 into crystalline Ta_2O_5. The heat generated due to the reaction can ignite the part and disintegrate the mold compound within. The phenomenon, which is referred to as "ignition failure," is usually accompanied by loud noise and possible flash. Ignition failure can occur under surge current conditions, for example when the tantalum capacitors are connected to a power supply in series. However, it is important to remember that ignition failure was initially activated by breakdown of the dielectric due to a voltage overstress rather than the high current inrush [3], [23]. Ignition failure of tantalum capacitors can be a serious concern for the product integrity, since it not only damages the part itself, but it also has the potential to damage other components, circuitry, and traces within its vicinity.

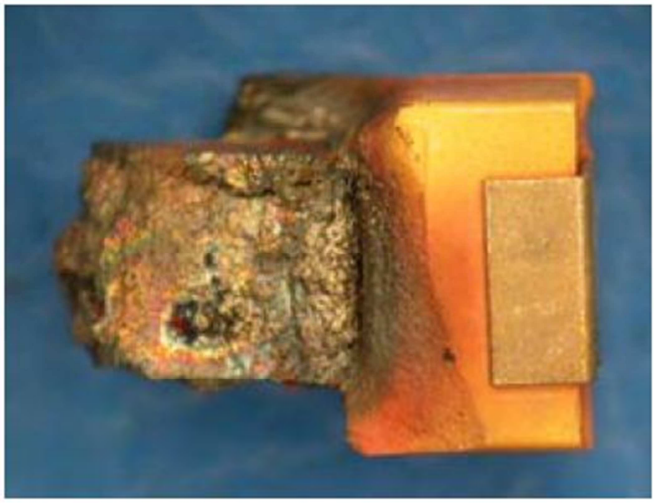

Figure 2: Ignition failure under surge current conditions that resulted in disintegration of tantalum capacitor [24].

1.1.3 Self-Healing of Tantalum Capacitors with Manganese Dioxide Cathodes

The self-healing mechanism is often cited as a feature contributing to the life of tantalum capacitors with manganese dioxide cathodes [3]–[5]. Self-healing can occur after a localized breakdown of the dielectric. Since breakdown sites form small current channels from the tantalum anode to the MnO_2 cathode material, the concentrated current causes a quick localized temperature rise in the MnO_2 cathode. If the temperature exceeds about 380°C [3], MnO_2 starts to release oxygen and converts to a reduced oxygen state with a lower conductivity. This process allows the cathode to isolate the failure by forming a Mn_2O_3 cap over the breakdown site (Figure 3). Self-healing requires a certain amount of time to take place [3]. Under large surge currents, there is not enough time for self-healing to take place [4], which is the reason why self-healing is not observed under surge current conditions. It should be noted that self-healing does not eliminate, but rather isolates the breakdown site. In the event of an incomplete self-healing process breakdown can occur at the same breakdown voltage, whereas it is assumed that the breakdown site healed completely if the sample breaks down at a higher voltage than the first breakdown event. The process of breakdown of the dielectric with subsequent self-healing is referred to as “scintillation” and can be enforced in appropriate testing methods.

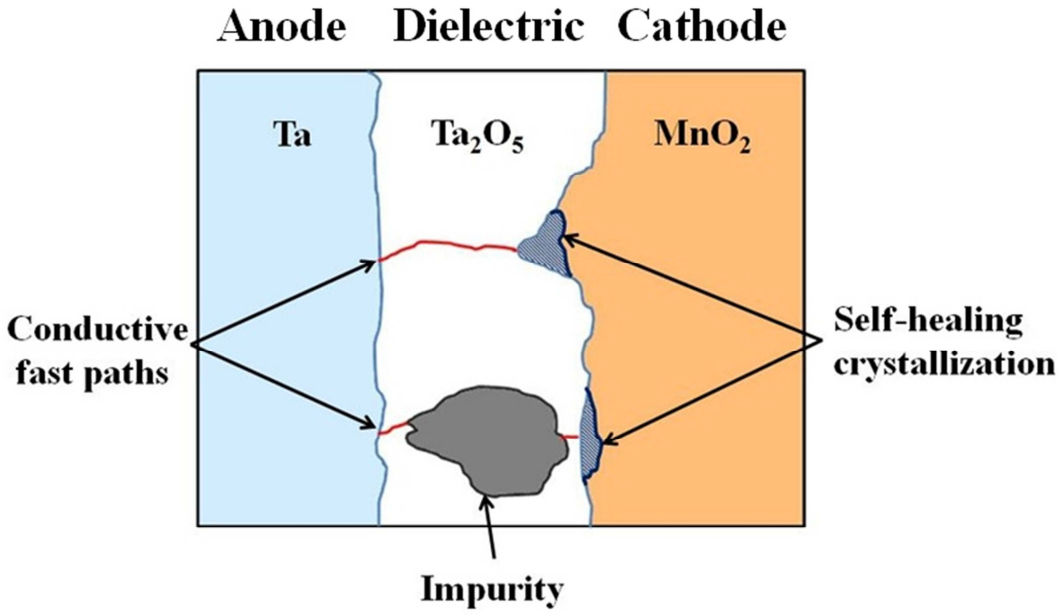

Figure 3: Schematic of self-healing after breakdown of the dielectric.

1.1.4 SCINTILLATION TESTING

Scintillation testing is used by capacitor manufacturers to assess the dielectric breakdown voltage between different lots and batches of capacitor populations and to deliberately activate the self-healing mechanism [3]. The method was initially introduced by Hewlett Packard to KEMET [3]. During scintillation testing, capacitors are slowly charged at a constant current, typically in the micro ampere range, while the voltage across the capacitor is measured (Figure 4). The capacitor under test is charged until breakdown of the dielectric occurs (Figure 5) or until the capacitor voltage is equal to a preset compliance voltage (V_C). After the breakdown the part discharges momentarily, which is observed as a sharp voltage drop (Figure 5). When the self-healing process is complete, the capacitor is able to charge again (Figure 6), which results in a measurable rise of voltage until the next breakdown occurs or until the compliance voltage is reached. If the compliance voltage is reached, the instrument switches from a constant current mode to a constant voltage mode in order to avoid voltage overstressing of the sample if needed (Figure 7). The voltage at which breakdown occurs in a scintillation test will be referred to as scintillation breakdown voltage (V_{Scint}).

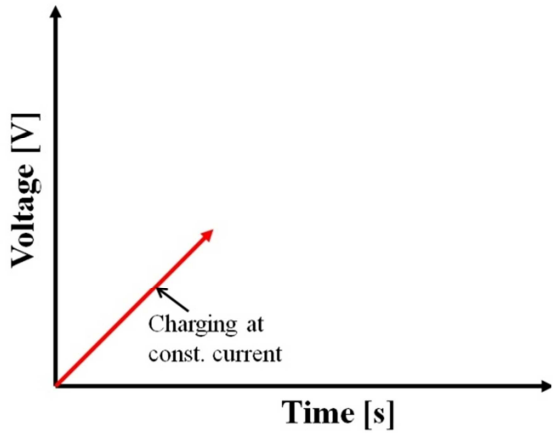

Figure 4: Slow charge at constant current in scintillation test.

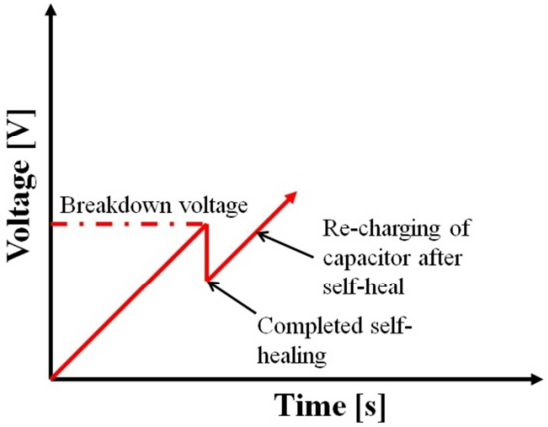

Figure 6: Activation of self-healing mechanism allows charging beyond breakdown voltage

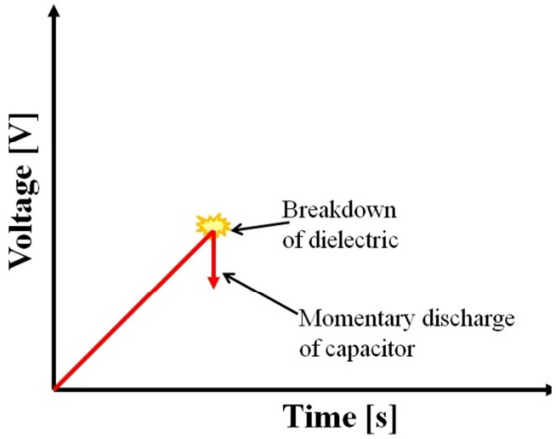

Figure 5: Dielectric breakdown followed by momentary discharge.

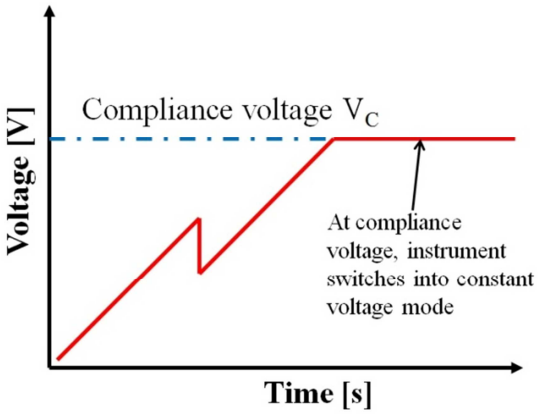

Figure 7: Compliance voltage limits voltage stress.

1.1.5 STEP STRESS SURGE TESTING (SSST)

In order to simulate power-on loading conditions as experienced by tantalum capacitors that are assembled in low impedance circuits, step stress surge current testing was developed. As opposed to scintillation testing, where breakdown of the dielectric can result in self-healing due to the low magnitude of the charging current, breakdown of the dielectric in surge testing results often in ignition failure. The high currents in SSST cause a rapid temperature increase after the breakdown event, which leads to ignition of the parts instead of self-healing. In the following chapters the voltage at which breakdown occurred in a SSST will be referred to as surge current breakdown voltage (V_{Surge}). SSST is used to assess the surge current capability of tantalum capacitors. [6], [23]–[26]. The test procedure is as follows: A large capacitor is charged to a set voltage level and subsequently discharged onto the device under test (DUT). The DUT is defined as failed if it did not charge to at least 90% of the set voltage level of the large capacitor. They cycle is repeated five times at one voltage level. If the DUT did not fail during the five cycles, the voltage level is increased by an increment that is dependent on the starting voltage, the expected breakdown voltage, and the required voltage failure resolution for the subsequent statistical analysis [23]. Previous work by Holland [27] shows that failure occurs at the first cycle when the dielectric strength is exceeded on the majority of tested samples. Similar observations were made by Teverovsky [28]. J. D. Prymak et al. [3], [23] believe that the voltage overstress triggers scintillations and surge current failures, suggesting that there should be no statistical significant difference between the breakdown voltage distributions of surge current and scintillation tested samples. Teverovsky [4], however, observed that the current magnitude affects the breakdown voltage level. He found lowered breakdown voltages for surge current tested samples as compared to scintillation tested samples.

1.1.6 MOTIVATION

Various screening methods are employed by capacitor manufacturers to ensure that the parts are capable of withstanding surge currents in their application conditions. Surge current screening or qualification was designed to minimize the failure under surge current conditions. However, the test as specified per MIL-PRF-55365 [29], is optional and usually only available for high reliability parts. Some manufacturers [11], [12] employ surge current screens on 100% of their industrial grade parts. Despite screening methods, failures during the power-on process of surge current screened tantalum capacitors were reported, even at voltages lower than their rated voltages [8]–[10]. The reason for the lowered failure voltages was believed to be an exacerbation or creation of defects in the dielectric due to thermo-mechanical stresses experienced during the reflow process. It was suggested that the risk of ignition failure is increased if voltage transients occur when switching on the power supply. Teverovsky [30] and Holland [27] showed that the circuit inductance can cause significant voltage overshooting of 70% above the intended application voltage. Teverovsky [4] indicated that the current magnitude had an effect on the breakdown voltage distribution. Comparing the breakdown voltage distribution of scintillation and surge current tested populations, he found that surge current tested breakdown voltages were lower. This was in contrast with the observation that Prymak and Marshall [3], [23] made, which lead them to believe that a voltage overstress activates the breakdown mechanism, while the current magnitude had an effect on the failure mode.

Surge current failures are believed to occur due to manufacturing defects and impurities that reduce the breakdown voltage to lower levels than the forming voltage [6], [7]. It was also suggested that the self-healing mechanism has the potential to clear out these defects as well as defects created by thermo-mechanical stresses during the reflow process [6]–[9].

In order to reduce failure under surge current conditions, a screening or conditioning method is needed, that effectively screens out weak samples or improves the surge current capability of the parts without having a detrimental effect on their reliability. The suggestions of other researchers indicated that

scintillation testing and its ability to deliberately activate the self-healing mechanism in tantalum capacitors with manganese dioxide cathode is able to clear out defects that would have resulted in an increased surge current failure risk in their application. This was further supported by our observations in preliminary experiments that showed that the deliberate activation of self-healing improved the breakdown voltage of weak parts that would otherwise have an increased risk of ignition failure. This improvement was expected to translate to a better performance under surge current conditions. Therefore we suggest a conditioning method based on scintillation testing, that either screens out samples that are not capable of a predetermined breakdown voltage or that conditions weak samples by activating the self-healing mechanism to improve their breakdown voltage. The improvement is expected to minimize failures under surge current conditions that otherwise would have failed, since the self-healing mechanism is not activated at high current levels. This study investigated the effect of self-healing on the leakage current and breakdown characteristics of tantalum capacitors and whether the improvements mitigated the risk of failure under surge current conditions. The benefits of the conditioning method were demonstrated in a surge current test with the objective of mitigating the surge current failures of tantalum capacitors with manganese dioxide cathodes. In addition a life test was conducted to address concerns of a reduced life of tantalum capacitors due to scintillation conditioning.

1.1.7 LITERATURE REVIEW

While it has been shown that the activation of the self-healing mechanism was possible with scintillation testing [3], [5], [31], research on the effect of self-healing on the electrical characteristics such as breakdown voltage and leakage current of the parts was limited. Teverovsky [5], [31] found that self-healing degraded the parts and, therefore, decreased the surge current failure voltages. He conducted scintillation tests with different capacitor types and recorded the scintillation breakdown voltages. The first two scintillation voltages were compared to identify whether the self-healing process was incomplete and therefore damaging. He distinguished between constructive and destructive scintillations based on the following definitions:

$$\boldsymbol{Constructive\ scintillation}: \boldsymbol{V_{Scint1} < V_{Scint2}} \quad \textbf{(2)}$$

$$\boldsymbol{Destructive\ scintillation}: \boldsymbol{V_{Scint1} > V_{Scint2}} \quad \textbf{(3)}$$

The definitions of V_{Scint1} and V_{Scint2} and examples of damaged and non-damaged parts are illustrated in Figure 8.

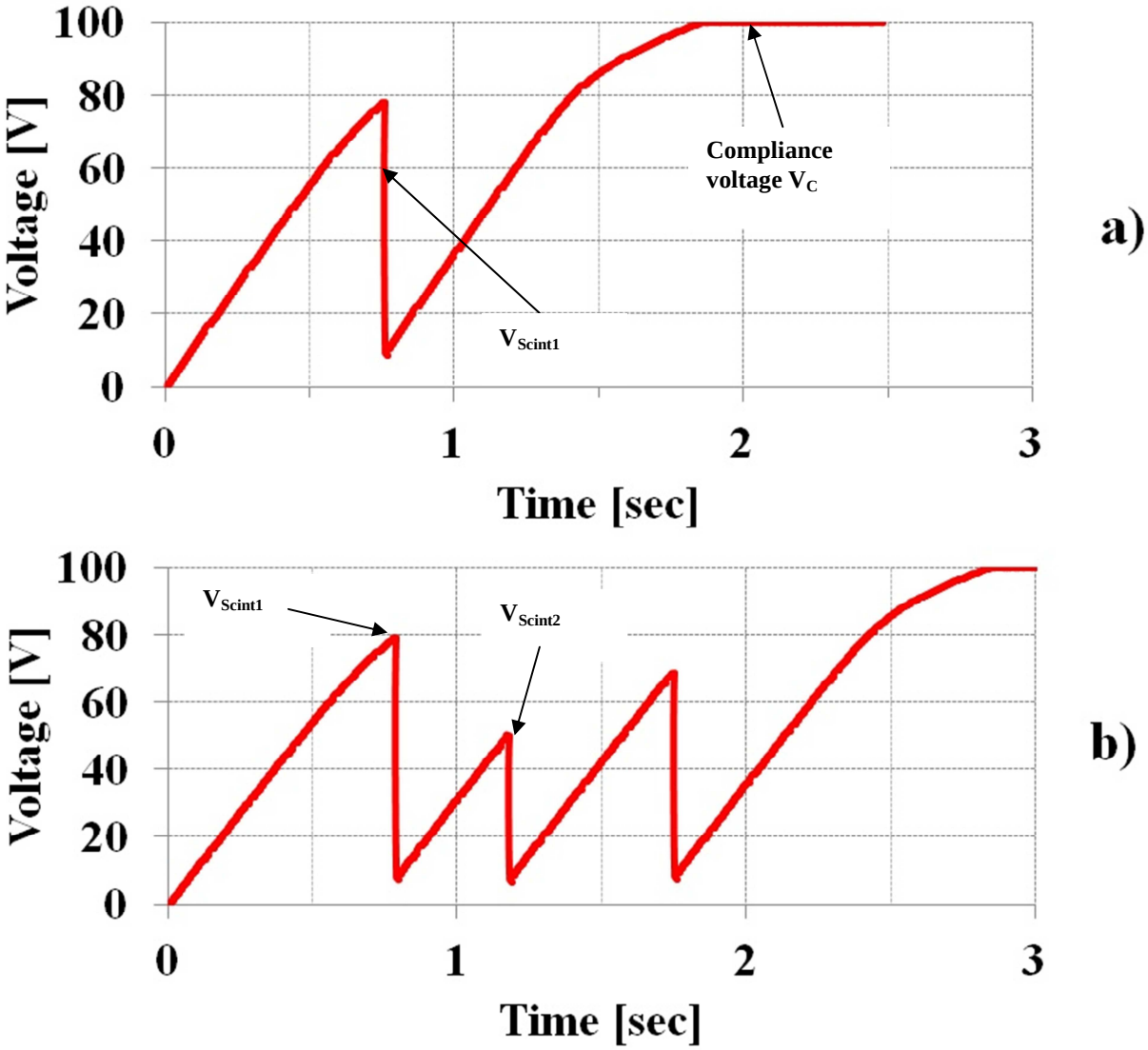

Figure 8: Examples of voltage behavior over time of scintillation tested tantalum capacitors.

Teverovsky [5], [31] found that the proportion of damaged capacitors that experienced multiple scintillations ranged from 0% to 100% depending on the lot, which degraded the parts and possibly have a detrimental effect on the surge current reliability of the parts. Teverovsky [4] also examined the effect of scintillation and step stress surge current testing on the breakdown distributions. The Weibull distributions of the breakdown voltages for scintillation and surge current tested samples were found to indicate similar breakdown mechanisms. This suggested that improvements due to self-healing in breakdown voltage under scintillation test conditions translate to improved breakdown voltages under surge current conditions without introducing new failure mechanisms. Teverovsky observed lower breakdown voltages for parts that were test under surge current conditions than under scintillation test conditions. This is contrary to Prymak et al. [3], [8], [23], who found that the current magnitude affects the occurrence of self-healing or ignition following the breakdown rather than the level of breakdown voltage.

Long et al. [8], [9] developed a method ("proofing") to improve the surge current performance of tantalum capacitors with MnO_2 cathodes. The method involved powering up capacitors through a 1000 Ω resistor and verifying the voltage across the capacitor after 7 seconds of an application of rated

voltage. If the voltage was not within 90% of the applied voltage the part was screened out. Comparison of proofed and non-proofed capacitor populations showed higher projected failure voltages under scintillation and surge current test conditions for the proofed populations. A life test at rated voltage and 85°C showed improved failure rates for the proofed populations. It was observed that proofing did result in a decreased failure rate in the proofed populations. The authors believed that self-healing during the proofing process might be the reason for the improved performance of the parts. The effect of self-healing on the life and surge current reliability is unknown, since possible self-healing events during the proofing process were not monitored. Therefore, the possible detrimental effects of incomplete self-healing need to be determined. In addition, screening out weak parts could be responsible for the longer life and better surge current reliability. Detailed analysis of the correlation between self-healing and the mitigation of surge current failure needs to be conducted. While the proofing method improved the surge current performance of tantalum capacitors, the risk of surge current failure can be further reduced with an efficient method that screens out incompletely self-healed parts.

1.2 EXPERIMENTAL WORK

1.2.1 APPROACH

Since self-healing can result in permanently damaged parts, it was important to identify the optimal parameter for scintillation conditioning. The most desirable outcome for scintillation conditioning was to maximize the number of self-healed and non-damaged samples. The charging current was believed to a critical parameter for the completion of self-healing. Therefore, various populations were exposed to varying charging current in the micro-amp range to identify the optimal conditions for self-healing for the subsequent conditioning process.
After the optimal charging current was identified, capacitor samples from two different manufacturers A and B were exposed to scintillation conditioning to deliberately activate the self-healing mechanism in weak samples among their population. Based on the literature review and our own observation we expected an improvement of the breakdown characteristics. In order to confirm our hypothesis the impact of the conditioning method on tantalum capacitors was assessed under two test conditions. In the first test conditioned and non-conditioned samples from both manufacturers were subjected to a step stress surge test to assess the breakdown voltages under surge current conditions. In a second test, the populations were exposed to a highly accelerated life test under accelerated voltage and temperature conditions. The intention of the life test was to demonstrate that the scintillation conditioning method did not have a detrimental effect on the life of the parts.

1.2.2 PREPARATION FOR SCINTILLATION CONDITIONING

Test samples with the same design parameters from two manufacturers were chosen for the tests. Both capacitor types were industrial standard, EIA size 2917 tantalum capacitors with MnO_2 cathodes. The characteristics of the capacitors are listed in Table 1.

Parameter	Specifications
Rated Voltage [V_{DC}]	**35**
Capacitance [µF]	**6.8**
Tolerance [%]	**10**
Temperature range [°C]	**-55 to +125**
Max. leakage current [µA]	**2.4**
Dissipation factor [-]	**0.06**
Max. equivalent series resistance @ 100 kHz [Ω]	**1.3**

Table 1: Electrical characteristics of tantalum capacitors tested in the study.

150 samples from each manufacturer were exposed to scintillation conditioning. Before the parts were exposed to any electrical or thermal stresses the parts were baked at 125°C to remove residual moisture from the package as described in JEDEC JESD22-A113D [32]. Rapid temperature changes as experienced in the reflow process or during scintillation events could cause expansion of the moisture within the package that could cause mechanical stresses, which could damage the dielectric. The standard required a minimum "bake out" time of 24 hours. We tracked weight changes of the samples in 12 hour intervals and found that the samples were not completely dried after 24 hour and required 48 hours as a minimum bake out time.

The impact of self-healing can be difficult to determine if the proportion of self-healed parts in the population is small or if the improvements in breakdown voltage (BDV) is small. The compliance voltage served as a cutoff separating the weak and nominal parts of the population. Therefore, an appropriate criterion for the compliance voltage had to be defined in order to condition the weak parts without overstressing the nominal parts. If the compliance voltage was chosen too high, not only the weak samples but also nominal samples of the population would have been exposed to scintillation. A compliance voltage was chosen that would result in a significant number of weak samples (15.8%) as shown in Figure 9.

The criterion for the compliance voltage was defined based on the mean and the standard deviation for the sample populations from both manufacturers as follows:

$$V_C = \mu_{Scint} - \sigma_{Scint} \qquad (4)$$

where V_C was the compliance voltage [V], μ_{Scint} was the mean of the scintillation breakdown voltage [V], and σ_{Scint} was the standard deviation of the scintillation breakdown voltages [V].

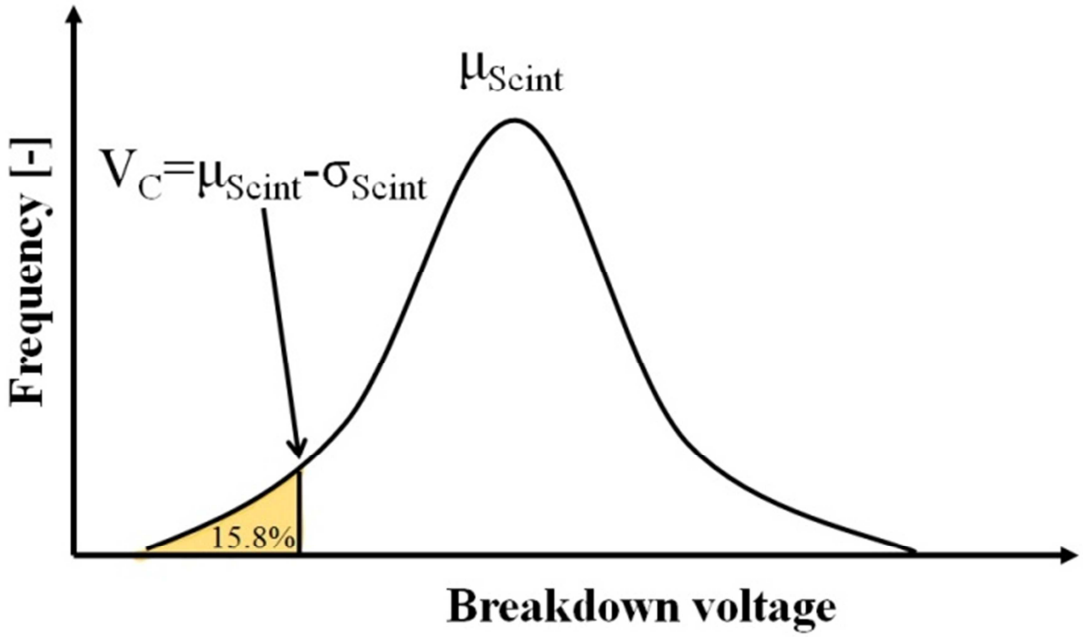

Figure 9: Effect of compliance voltage selection on percentage of self-healed parts.

Assessment of the breakdown voltage distributions was used to determine the quality variations between different capacitor lots. In order to identify the breakdown voltage distribution for the two capacitor types used in this study, groups of 30 capacitors from each manufacturer were scintillation tested to measure the breakdown voltage. The mean (μ_{Scint}), standard deviation (σ_{Scint}), and scintillation breakdown voltage for each population were calculated.

Based on the definition of the criterion of compliance voltage, we expected that 15.8% of our samples that were exposed to scintillation conditioning will either be scintillation conditioned or screened out if the self-healing process was incomplete.

The results from the initial assessment of the scintillation voltage distributions of capacitors from manufacturers A and B (each n=30), and their respective compliance voltages as used in the scintillation conditioning procedure are summarized in Table 2:

Manufacturer	**A**	**B**
μ_{Scint} [V]	**79.60**	**80.70**
σ_{Scint} [V]	**4.72**	**20.88**
V_C [V]	**74.88**	**59.82**

Table 2: Mean and standard deviation as measured for n=30 samples from manufacturer A and B in order to determine compliance voltage for the subsequent scintillation conditioning method.

The breakdown voltage distributions and the compliance voltage are shown in Figure 10 and Figure 11.

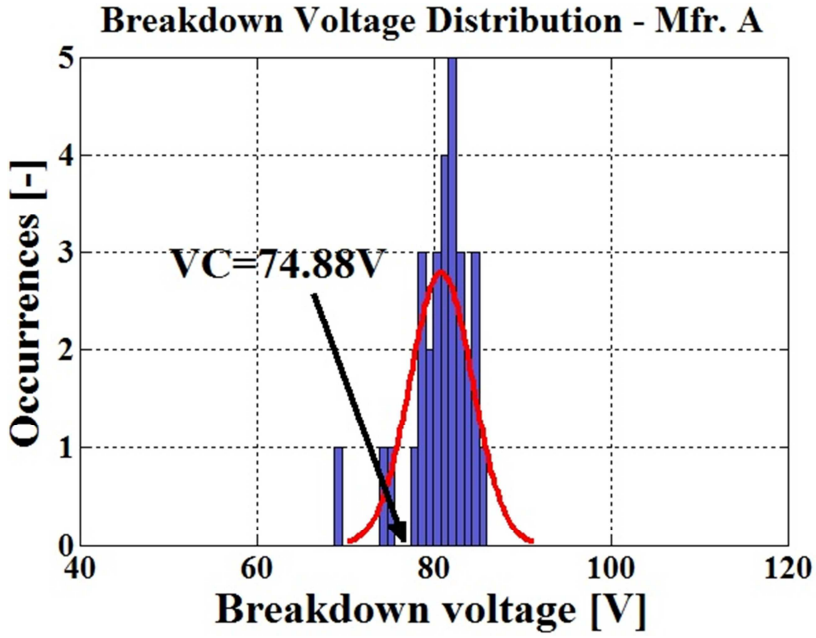

Figure 10: Distribution of breakdown voltages of parts from manufacturer A.

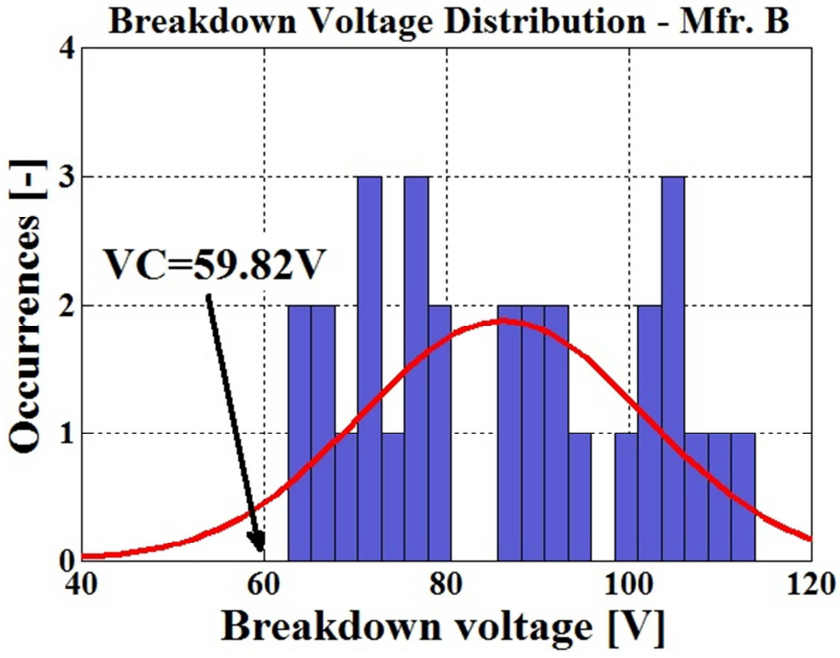

Figure 11: Distribution of breakdown voltages of parts from manufacturer B.

The results revealed differences in the quality control between the two manufacturer lots. Variations of the breakdown voltage of a capacitor population can be attributed to manufacturing variations in the dielectric thickness or impurities embedded in the dielectric layer among others. The margins between the compliance voltages and the means of the breakdown voltages suggested that the potential breakdown voltage increase of weak samples was higher in the manufacturer B population as compared to manufacturer A. Therefore, the measurable effect of scintillation conditioning on the surge current reliability might be larger in the population of manufacturer B, where weak samples tended to break down at low breakdown voltage levels.

The parts were then conditioned at a temperature of 25°C and a charging current of 750 µA. To assess the effect of scintillation conditioning on the leakage current, the leakage current of each part was measured before (LC_{Pre} and LC_{Post}) and after conditioning after electrification with rated voltage for 5 minutes. Leakage current is an indicator of life degradation and is used in highly accelerated life tests (HALT) [5], [8], [15], [24], [28], [29], [33], which allowed us to identify possible degradation of the samples due to scintillation conditioning. A criterion solely based on a comparison of scintillation voltages as proposed by Teverovsky [5], [31] might not have reveal degradation of the capacitors in the event of incomplete self-healing. The outcomes of scintillation conditioning were a complete self-heal, an incomplete self-healing process, or no scintillation event for parts with a higher breakdown voltage than the compliance voltage. The two self-healing events could be identified by measuring the first scintillation voltage V_{Scint1} and the second scintillation voltage V_{Scint2}, if scintillations occurred. The part was considered as not completely healed and therefore damaged if the second scintillation voltage was lower than the first one. Analogous, the part was considered as self-healed if the second scintillation voltage was higher than the first one. The capacitor samples were accepted if both of the following criteria applied or if the capacitor sample charged up to compliance voltage without any scintillation:

$$\mathbf{LC_{Post} < 2LC_{Pre}} \quad (5)$$

$$\mathbf{V_{Scint_n} > V_{Scint_{n-1}}} \quad (6)$$

Possible outcomes of scintillation conditioning are demonstrated in Figure 12.

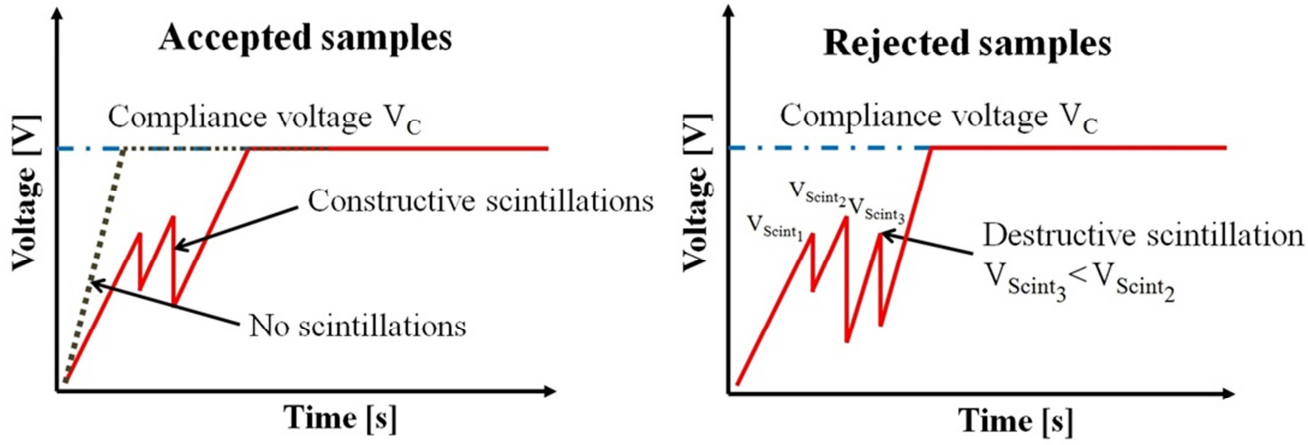

Figure 12: Schematic of scintillations of accepted and rejected samples.

1.2.3 RESULTS OF SCINTILLATION CONDITIONING

A summary of the percentages of screened out, self-healed, and passed samples is shown in Figure 13.

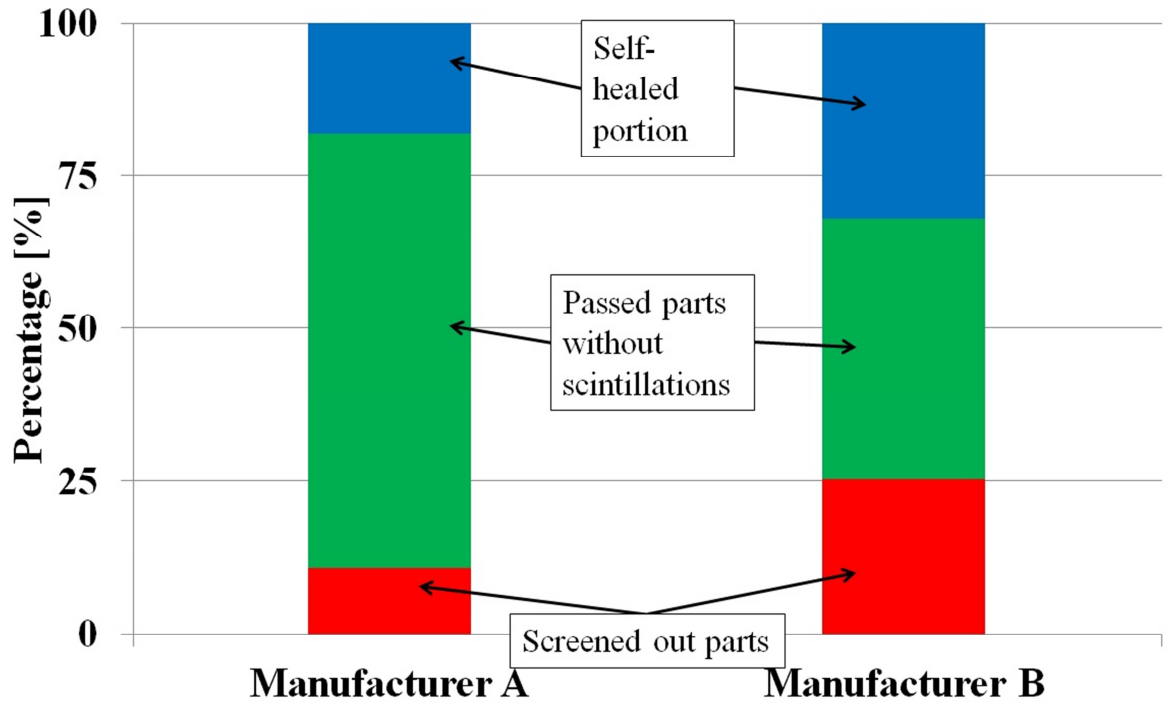

Figure 13: Percentages of parts that were screened out, self-healed, and passed without scintillations.

28% of the manufacturer A and 57% of the manufacturer B samples experienced scintillations. The percentages of rejected parts were significantly higher than the expected 18.6% as defined by the compliance voltage due to the conservative acceptance criteria. Parts were screened out if the leakage current increased by more than twice the original value. Most parts were found to be in the lower nano ampere range where a twofold increase should not have been problematic, since manufacturers specified the maximum leakage current at 2.4 µA. In this study the leakage current criterion for acceptance was conservatively chosen. Therefore, a less stringent acceptance criterion for leakage current would have resulted in a lower number of rejected parts without a detrimental effect on the sample population. In addition, choosing an appropriate compliance voltage for the manufacturing environment could have resulted in significantly different result. We considered 15.8% of the samples as weak in this study, which was significantly higher than what to expect from manufacturing processes, where the proportions of weak samples often fall into the ppt (parts per thousand) or ppm (parts per million) range.
The effect of self-healing on the scintillation breakdown voltage and leakage current was assessed after conditioning the parts. Changes in the scintillation breakdown voltage and the leakage current were only observed in parts that experienced scintillations. Parts that charged up to compliance voltage without scintillations showed no change in breakdown voltage or leakage current. To determine the scintillation breakdown increase due to scintillation conditioning the first scintillation breakdown V_{Scint1} was compared to the respective compliance voltage of each manufacturer. A summary of the average change of breakdown voltage and leakage current in parts is shown in Figure 14.

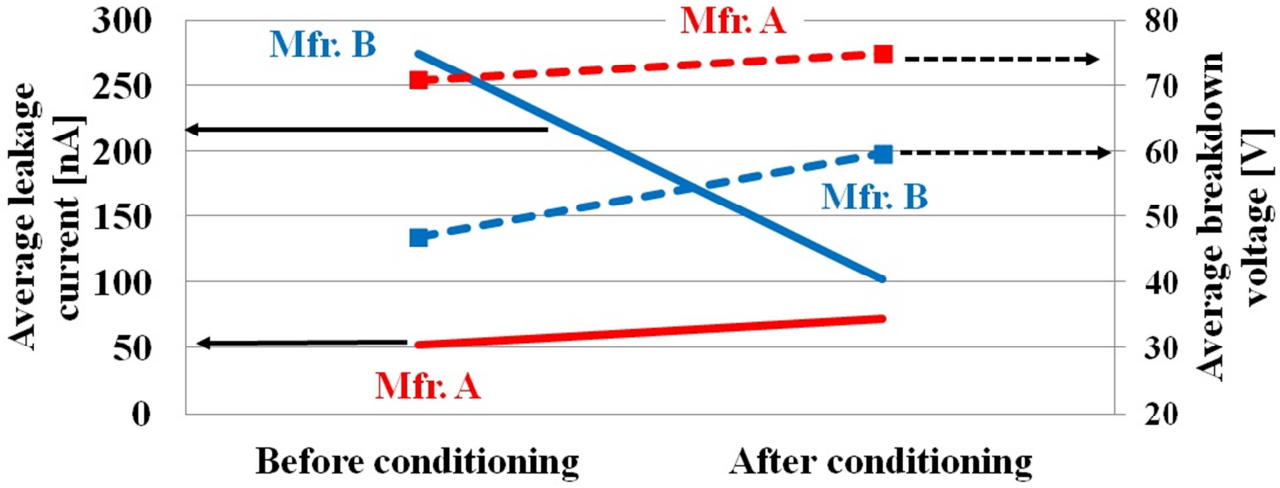

Figure 14: Effect of scintillation conditioning on average breakdown voltage and average leakage current.

The average scintillation breakdown voltage increased by 5% in parts from manufacturer A and by 27% for parts from manufacturer B. This behavior was in agreement with the analysis of the breakdown voltage distributions, which showed a larger standard deviation for the manufacturer B lot. Weak samples of manufacturer B exhibited a larger potential increase of breakdown voltage due to scintillation conditioning. The improved breakdown voltages achieved under scintillation test conditions were expected to translate to an improved surge current reliability.
A table showing the changes in leakage current and breakdown voltage (BDV) is presented in Table 3.

	Percentage change [%]	
	BDV	**Leakage current**
Manufacturer A	**>5.69**	**37.09**
Manufacturer B	**>27.21**	**-62.84**

Table 3: Summary of percentage change of leakage current and breakdown voltage of self-healed parts after scintillation conditioning.

The increase of breakdown voltage was higher in self-healed parts from manufacturer B. Weak parts from manufacturer B showed an average increase of breakdown voltage of about 27%, whereas the average increase of breakdown voltage in parts from manufacturer A was about 6%. This increase was expected to be reflected in the step stress surge test, since breakdown under surge current conditions is equally triggered by a voltage overstress as under scintillation test conditions [3], [23]. In addition, leakage current has been established as the most sensitive indicator of degradation of tantalum capacitors and is therefore commonly used as a failure criteria in highly accelerated life tests [5], [8], [15], [24], [28], [29], [33]. Since a breakdown of a dielectric results not only resulted in a drop of voltage, but also in a sharp increase of leakage current, a comparison of leakage current before and after scintillation conditioning was used to identify any detrimental effects of self-healing, which a comparison of scintillation voltages as proposed by Teverovsky [5], [31] might not reveal. Our results showed only a slight decrease or increase of leakage current after self-healing. Scintillation conditioning resulted in a 37% increase of leakage current of manufacturer A parts. Given the low magnitude of leakage current in the nanoampere range (μ_{LC_A}=39.87nA) before exposing the samples to scintillation conditioning, a 37% increase was still order of magnitudes lower than the manufacturers failure criterion

of leakage current at 2.4 μA or could have been due to variation of the measurement. A detrimental effect on the life of the parts was therefore not expected. Contrary observations were made for self-healed parts from manufacturer B. The parts showed higher leakage currents before scintillation conditioning with a mean of μ_{LC_B}=178.3 nA and showed a decrease of about 63% after scintillation conditioning. We observed that scintillation conditioning was able to reduce leakage current especially in outliers with a higher leakage current of up to 1.2 μA, while to parts with lower leakage currents were not as significantly effect by the self-healing process in terms of leakage current.
While most conditioned samples showed no degradation of leakage current, 12 screened out samples from manufacturer A and 4 screened out samples from manufacturer B showed a significant increase of leakage current of up to 12 times the original leakage current despite the occurrence of constructive scintillations, which was previously used by Teverovsky [5], [31] as the sole acceptance criteria. This showed that assessing the effect of self-healing based on scintillation voltages was not sufficient, since leakage current was shown to degrade even in cases where constructive scintillations were observed.

1.2.4 Assessment Of Effect of Scintillation Conditioning on Life Of Tantalum Capacitors With MnO_2 Cathodes

1.2.4.1 Experimental Setup And Procedures

The effect of the scintillation conditioning method on the life of the parts was assessed in a highly accelerated life test. While no detrimental effects were expected, based on the results obtained in Table 3, a life test had to be conducted to exclude the possibility of life degradation due to scintillation conditioning. Therefore the parts rated at 35V were exposed to accelerated voltage and temperature stress conditions. As defined per Weibull grading test in the military performance specification [29], the parts were stressed at 1.5 times the rated voltage (V_R) at 52V. However, we increased the temperature from 85°C to 125°C in order to reduce the testing time. Concerns that this might have caused the parts to fail due to other failure mechanisms can be refuted based on the observations of other researchers [5], [15], [28], [33] that raised the temperature up to 165°C and voltages up to $3xV_R$ without observing new failure mechanisms. The test samples were divided into two sub-groups, consisting of conditioned and non-conditioned samples. Each group contains sub-groups from two different manufacturers. An illustration of the individual groups is shown in Table 4.

	Manufacturer A	**Manufacturer B**
Conditioned	**25**	**25**
Non-conditioned	**24**	**25**

Table 4: Sample size in each in HALT test.

The sample size was limited to about 25 samples each due to the design restrictions of the test boards. The samples were reflowed with 96.5Sn3.5Ag solder with a peak temperature of 225°C onto test boards with 25 samples. The samples were connected with fast acting fuses rated to 125 mA in series, since leakage current was identified as the most sensitive indicator of tantalum capacitor degradation, and was used previously as failure criteria in life tests [5], [8], [15], [24], [28], [29], [33]. The power supply used in the test was capable of providing up to 52V and 35A, which was sufficient to supply the current of 0.35A that was necessary to blow up the fuses in 0.01 sec as specified by their specification sheet. The

fuses were placed outside the chamber. The voltage drop across the fuses was continuously monitored at 3 minute intervals using the Agilent 34980A Benchlink data logger software. Failure was detected and the time to failure was recorded when the fuses blew up and the voltage drop increased to more than 50 V. A test board schematic is shown in Figure 15.

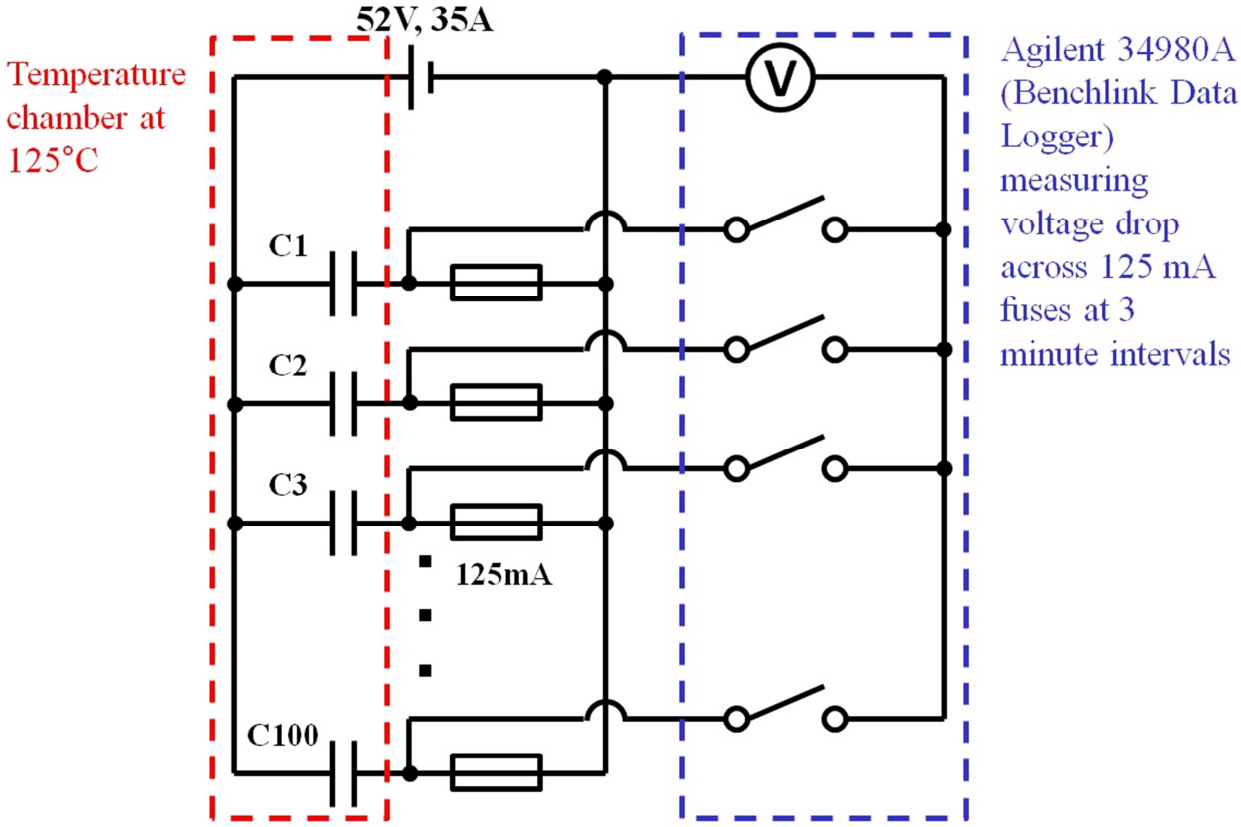

Figure 15: Schematic of test circuit of life test at 125°C and 52V.

1.2.4.2 Results of Highly Accelerated Life Test

The failure data of the life test for the conditioned and non-conditioned populations was analyzed in Reliasoft Weibull++™. Analysis for the manufacturer A populations showed bi-modal distributions as shown in Figure 16. While the failure mechanisms were not affected by the conditioning method, we observed a slightly higher η value for the conditioned population. This suggested that scintillation conditioning had no detrimental effect, but instead improved the life of the population. One infant mortality failure in the conditioned population was observed. A closer look at this data point revealed that the infant mortality failure was not due to an activation of the self-healing mechanism, since the sample charged to the compliance voltage without the occurrence of scintillations.

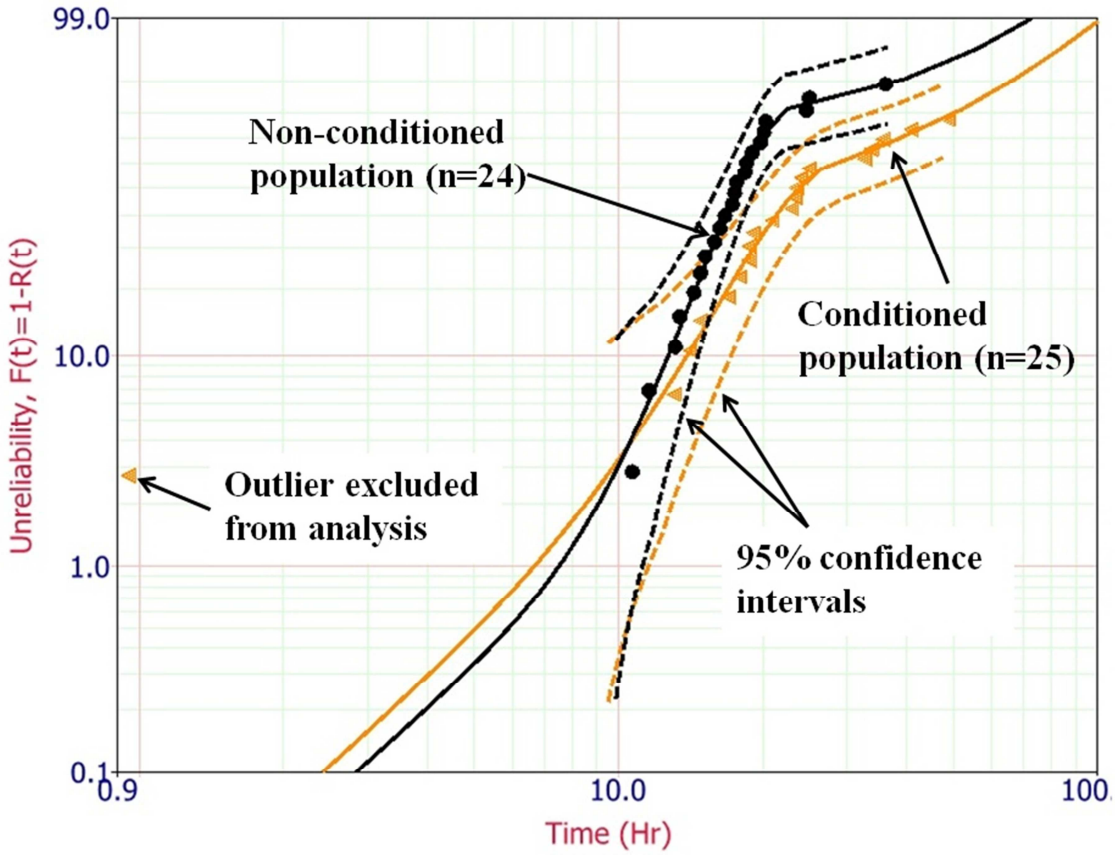

Figure 16: Life test results for the conditioned and non-conditioned population from manufacturer A.

The life test of manufacturer B (Figure 17) populations did not result in a significant number of failed samples. Most failures were infant mortality failures that occurred within 1 hour. While no conclusions about the life of the samples could be drawn due to the limited statistical information, we observed a higher number of infant mortality failures in the non-conditioned population. This indicated a positive effect of scintillation conditioning on the manufacturer B population. Surprisingly, even after testing up to 4000 hours no wear out mechanism was observed. Teverovsky [5] made similar observations and found that testing different capacitor designs at the same conditions resulted in a significantly different characteristic life with some capacitor lots showing no wear out mechanism. A summary of the estimated Weibull parameters is shown in Table 5.

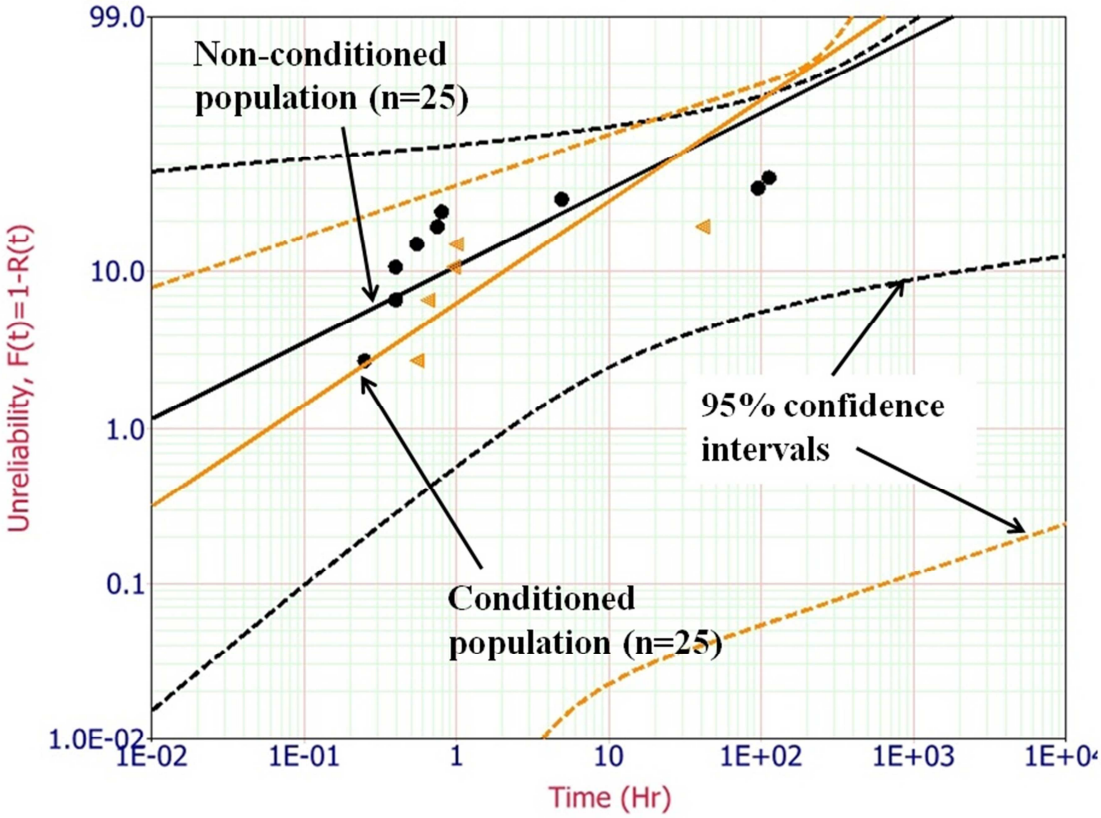

Figure 17: Life test results for the conditioned and non-conditioned population from manufacturer B.

		β1	η1 [hr]	β2	η2 [hr]	Correlation coefficient ρ	Number of samples	Failures
Mfr. A	Non-conditioned	6.47	17.85	2.04	41.41	0.917	24	22
	Conditioned	4.69	20.92	2.04	51.05	0.912	25	19
Mfr. B	Non-conditioned	0.49	82.23	-	-	0.700	25	9
	Conditioned	0.66	63.74	-	-	0.666	25	5

Table 5: Estimated Weibull parameters of HALT test.

No statistical differences were observed between the respective populations of manufacturer A and B. This meant that there was no evidence for the concern that scintillation conditioning degraded the life of the parts. Instead the data indicated that an improvement in the life was achieved in the manufacturer A population. The behavior of the capacitor population from manufacturer A and B in the life test was inconsistent. While the statistical analysis of manufacturer A data revealed a wear out mechanism, parts from manufacturer B failed due to infant mortality. Testing of the manufacturer B population was continued but no additional failures were observed.

1.2.5 Assessment Of Effect of Scintillation Conditioning on Surge Current Breakdown Behavior Of Tantalum Capacitors With MnO_2 Cathodes

1.2.5.1 Experimental Setup And Procedures

In order to assess the effect of scintillation conditioning on the surge current reliability of the parts a step stress surge current test (SSST) was conducted. The test was designed to simulate power-on loading conditions as experienced by tantalum capacitors in low-impedance circuits [6], [23]–[26]. In surge testing, dielectric breakdown often results in ignition failure as opposed to self-healing during scintillation conditioning. Analogous to the life test, the test samples were divided into two sub-groups, consisting of non-conditioned and conditioned samples. Each group contained sub-groups from two different manufacturers. A summarizing table is shown in Table 6.

	Manufacturer A	Manufacturer B
Conditioned	26	24
Non-conditioned	24	19

Table 6: Sample size in each group in surge current reliability test.

The underlying concept of the test was to charge the samples to preset voltage levels in the shortest time possible. This was accomplished by charging a large capacitor the desired voltage and discharging it onto the DUT with a relay or a MOSFET (metal–oxide–semiconductor field-effect transistor). Not only the various resistive, inductive, and capacitive elements, but also the switch type has a significant effect on the stress experienced by the DUT. Teverovsky studied the effect of inductive, resistive, capacitive,

and switching elements on the surge current test [30] in order to provide recommendations that can improve the reproducibility of surge current testing.
A schematic of the stress step surge test setup is shown in Figure 18.

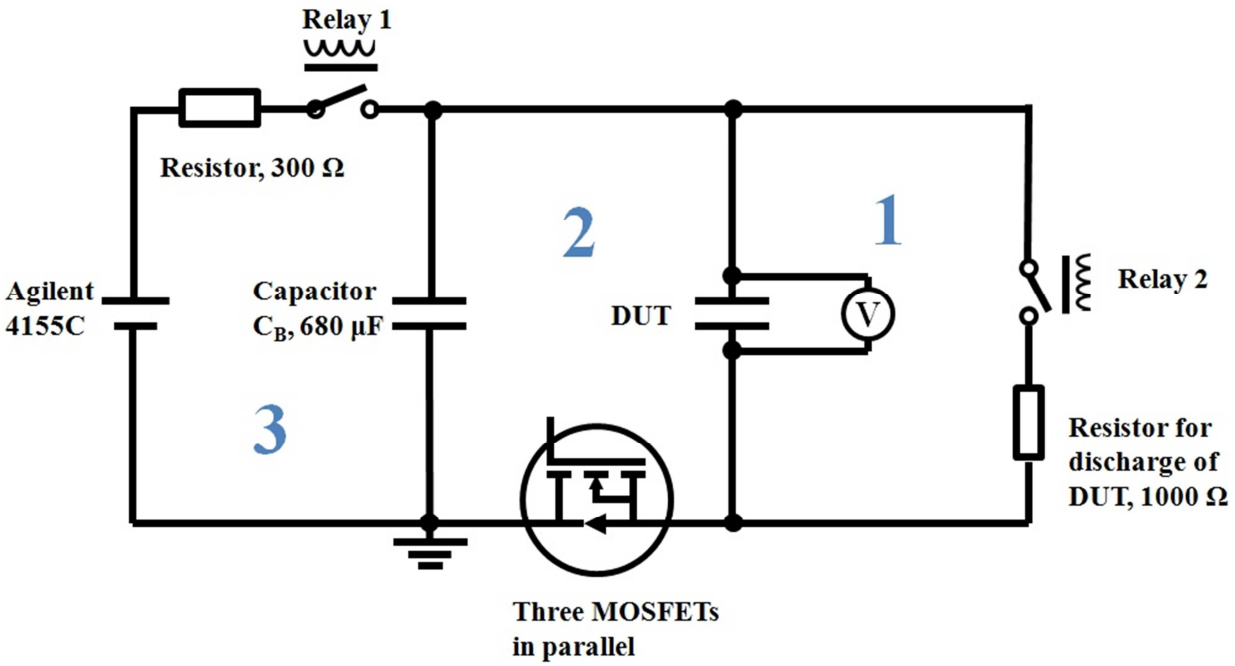

Figure 18: Test circuit of step stress surge current setup.

The test circuit consisted of basically three individual circuits labeled as 1, 2, and 3 in the test schematic. Initially, the DUT was discharged over a 1000 Ω resistor in circuit 1 for 10 sec by closing relay 2. After the DUT was fully discharged, the large capacitor C_B was charged to rated voltage of the DUT over a 300Ω resistor in circuit 3. A voltage was applied by the voltage source Agilent 4155C after relay 1 was switched. After charging capacitor C_B for 4 seconds to ensure that it reached the preset voltage level, relay 1 was opened. In the final step the DUT was quickly charged by capacitor CB by switching three parallel MOSFETs in circuit 2. The voltage drop across the DUT was measured with an oscilloscope when the MOSFETs were switched. If the DUT did not fail at the rated voltage, Capacitor C_B was charged to a higher voltage at 1V increments until failure occured. An example of recorded voltage drops across DUTs after the MOSFETs were switched on is shown in Figure 19.

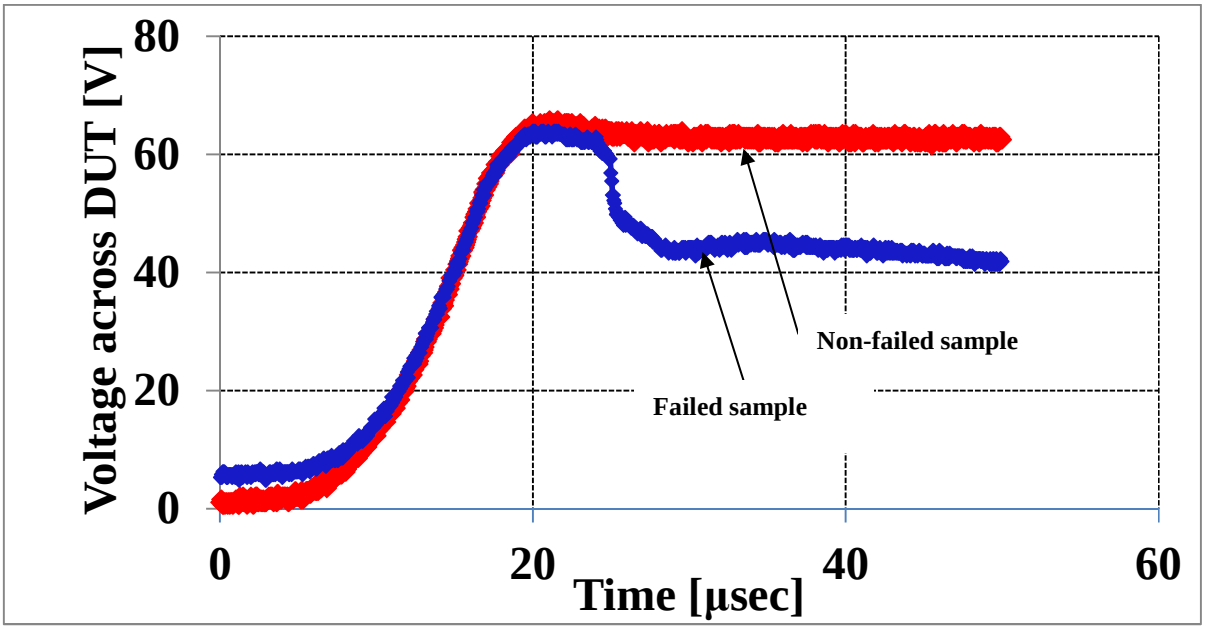

Figure 19: Typical voltage behavior in surge current test recorded with an oscilloscope. Failed and non-sample are shown at the same voltage stress level.

A capacitor failed if the voltage level after 50 µsec was not within 10% of the applied voltage stress level. If failure occurred, the voltage level was recorded. The Agilent 4155C instrument was used to provide the voltage to capacitor C_B, as well as the gate voltages for the relays and MOSFETs. A LabVIEW program was written to perform the described tasks automatically. A limitation of the equipment was the maximum voltage stress level of 100 V. If the DUT did not failed at this level, the sample was labeled as non-failed and suspended at 100V.

1.2.5.2 Results of Surge Current Reliability Test

The failure data was analyzed in Reliasoft Weibull++™. A two-parameter Weibull distribution provided a good fit to the data as shown in Figure 20 and Figure 21.

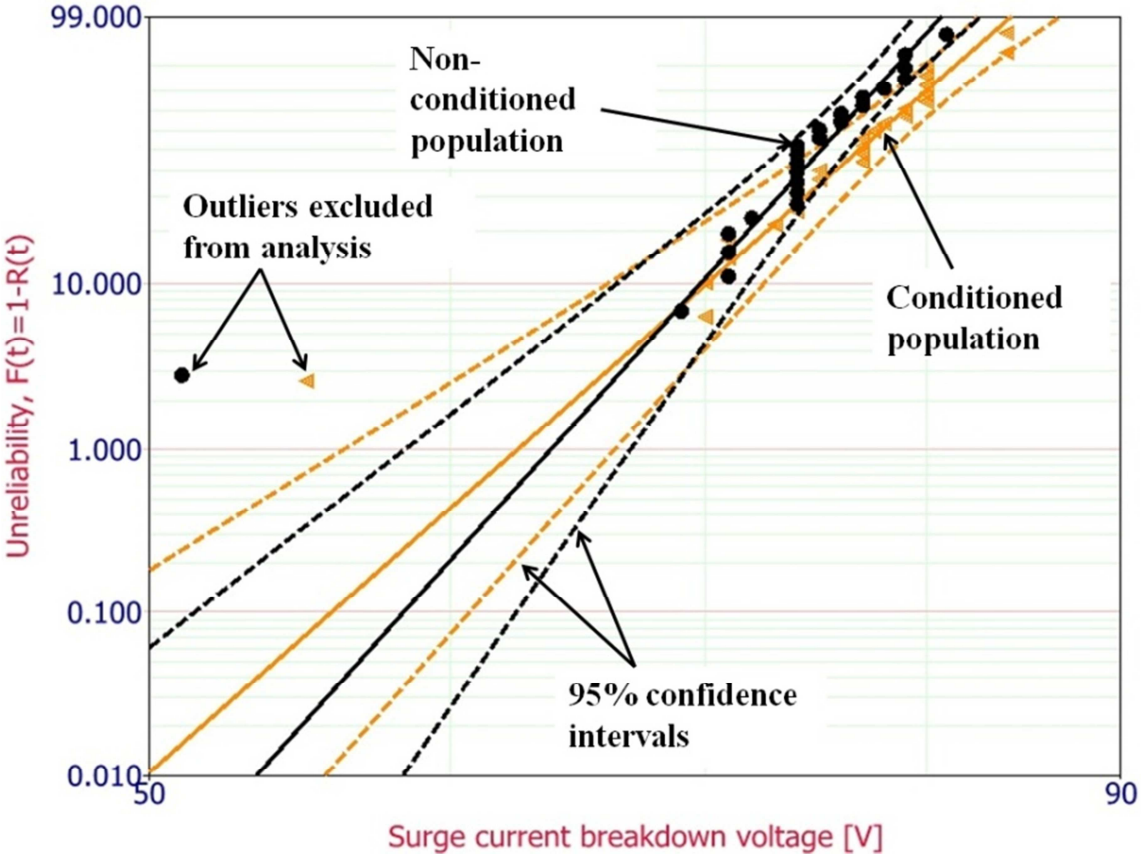

Figure 20: Two-parameter Weibull analysis of step stress surge current test data of conditioned and non-conditioned samples from manufacturer A.

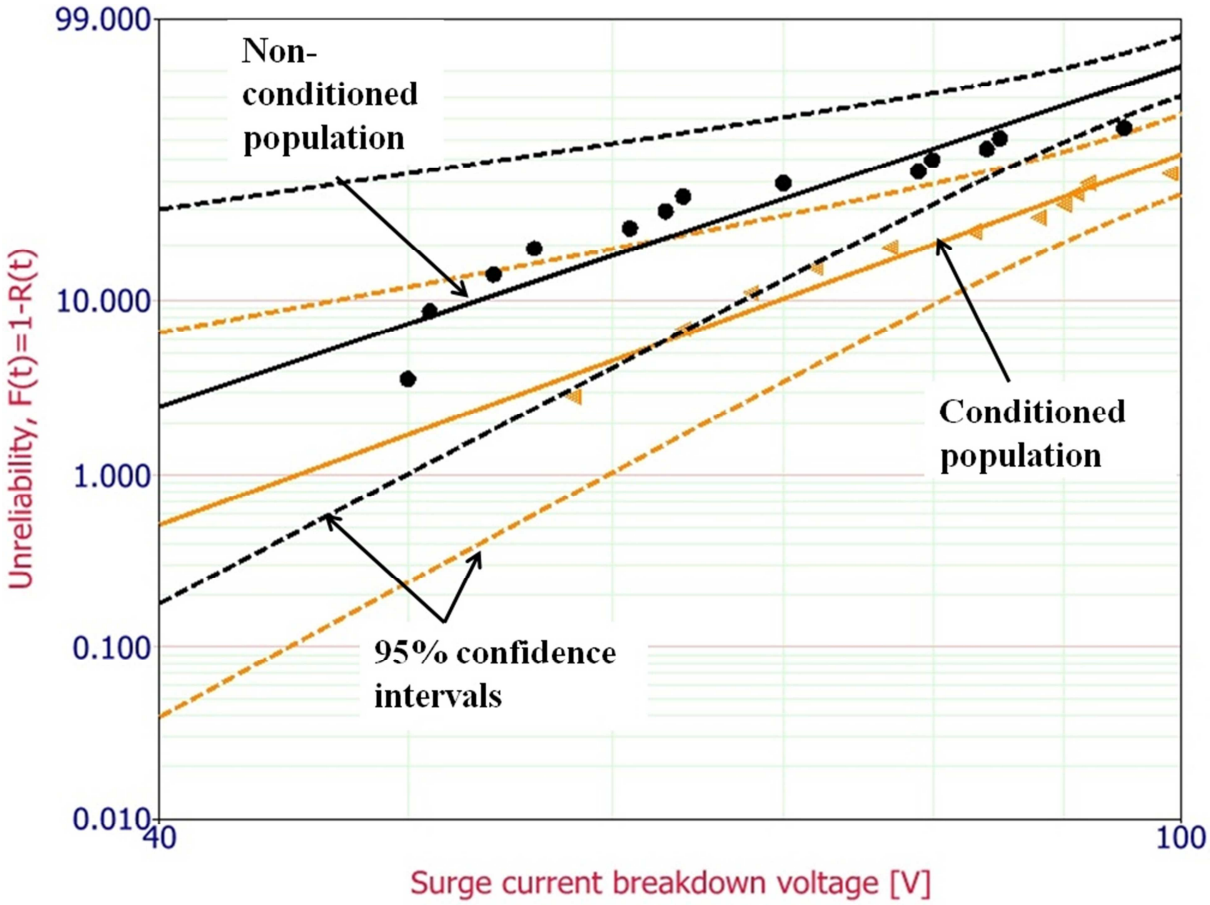

Figure 21: Two-parameter Weibull analysis of step stress surge current test data of conditioned and non-conditioned samples from manufacturer B.

The Weibull parameters and correlation coefficients of the analysis are summarized in Table 7:

		β	η [V]	Correlation coefficient ρ	Number of samples	Suspended samples at 100 V
Mfr. A	**Non-conditioned**	**25.91**	**76.12**	**0.98**	**24**	**0**
	Conditioned	**20.5**	**78.18**	**0.98**	**26**	**0**
Mfr. B	**Non-conditioned**	**4.99**	**83.61**	**0.93**	**19**	**6**
	Conditioned	**5.43**	**105.49**	**0.98**	**24**	**13**

Table 7: Estimated Weibull parameters of step stress surge current test.

The 27% BDV increase due to scintillation conditioning was close to the 26% surge current BDV increase of manufacturer A. Similarly, the difference between the scintillation BDV increase of 5% and the surge current BDV increase of 3% was marginal. This demonstrated that scintillation conditioning was effective in mitigating surge current failures. We observed that the breakdown voltage improvement in the population of manufacturer A was small compared to the population of manufacturer B. This suggested that scintillation conditioning should primarily be applied to populations or lots with a high BDV standard deviation, where an improvement in surge current breakdown voltage of weak samples had a significant effect on the population. While the overall breakdown voltage improvement in manufacturer B parts was about 26%, individual weak samples showed improvements of more than 100%. The beta values for the conditioned and non-conditioned populations indicated the same failure mechanisms, suggesting that no new failure mechanisms were introduced due to scintillation conditioning.

1.3 SUMMARY AND CONCLUSIONS

The impact of failure of tantalum capacitors with manganese dioxide cathodes under surge conditions can be catastrophic to the surrounding circuitry and components. Prymak et al. [8]–[10] showed that current screening tests did not reliably screen out weak samples, which resulted in reports of surge current failures. This study demonstrated that the deliberate activation of the self-healing mechanism can be used to improve the surge current reliability. The impact of scintillation conditioning on two competing capacitor designs was assessed in an accelerated life test at 125°C and $1.5xV_R$ of conditioned and non-conditioned samples. The results of the life test showed that scintillation conditioning did not degrade the life of the parts.

To assess the impact on the surge current reliability, we exposed conditioned and non-conditioned tantalum capacitor populations from both manufacturers to a step stress surge current test. The results showed that scintillation conditioning mitigates the ignition failure risk of tantalum capacitors. In the weaker population of manufacturer B the surge current breakdown voltage of the conditioned parts increased by 26% as compared to the non-conditioned parts. Individual weak samples showed improved surge current breakdown voltages by more than 100%. Further, we demonstrated that improvements due to self-healing in breakdown voltage under scintillation test conditions translate to improved breakdown voltages under surge current conditions.

To identify a possible detrimental effect of self-healing on the parts, leakage current and breakdown voltage was measured before and after conditioning. The analysis demonstrated that incomplete self-healing can degrade leakage current, while having no detrimental effect on the breakdown voltage, and must therefore be used as a screening criterion when assessing scintillation conditioned parts.
To expand the application range of tantalum capacitors with manganese dioxide, capacitor manufacturers drive current technology towards a higher voltage level, which increases the released energy in the event of surge current failure and the potential damage to the circuit. This development requires effective methods to reduce the ignition failure risk in weak tantalum capacitor populations. Scintillation conditioning proved to reduce the risk of failure under surge current conditions and can save the industry the cost of replacing damaged circuits due to ignition of tantalum capacitors.

1.4 RECOMMENDED FUTURE WORK

In order to confirm the hypothesis that new failure mechanisms were not introduced due to scintillation conditioning, physical evidence in the form of failure analysis of conditioned and non-conditioned samples should be provided.
If needed, the study should be expanded to a larger sample size while reducing the compliance voltage to reduce the number of weak samples that are exposed to scintillations. The lower percentage of weak samples would resemble manufacturing requirements, where the percentage of weak samples is usually significantly lower than in this study.
Further, in this study samples that experienced destructive scintillations were screened out even if the subsequent scintillations were constructive. Therefore, an effort should be made to analyze how destructive scintillations affect the capacitor performance, if the capacitor sample is able to finally charge up to the compliance voltage.

1.5 CONTRIBUTIONS

The study described in the thesis examined the effect of the deliberate activation of self-healing and its effect on the life and surge current test behavior of tantalum capacitors with manganese dioxide cathodes. The objective was to reduce surge current ignition failure that could result in significant damage on the PCB assemblies.
The contributions were as follows:

- Developed a scintillation conditioning method, which screens out incompletely self-healed parts. The procedure mitigates the risk of surge current failure of tantalum capacitors in field applications.
- Demonstrated that improvements due to self-healing in *breakdown voltage under scintillation test conditions* translated to improved *breakdown voltages under surge current conditions*, without harmful effects on the life of the parts.
- Demonstrated that incomplete self-healing can degrade leakage current and must be used as a screening criterion when assessing scintillation conditioned parts.

2 CHAPTER 2: EFFECTS OF STEP-STRESS TESTING AND TEMPERATURE CYCLING ON TANTALUM CAPACITORS WITH MnO_2 CATHODE

2.1 INTRODUCTION

Tantalum capacitors are widely used in the electronics industry. Comparing the characteristics of solid tantalum capacitors to competing capacitor technologies, one will find that tantalum capacitors offer an excellent volumetric efficiency (capacitance per volume), stability of electrical parameters over their specified voltage and temperature range, and high reliability. The reliability of tantalum capacitors is, however, tempered by the catastrophic failure mode of shorting, which can result in the ignition of the parts, and can severely damage components and structures in their vicinity. The current qualification procedures of capacitor manufacturers include testing of the parts at rated voltage and elevated temperatures for 2000 hours [34] [11]. Temperature cycling is tested in accordance with MIL-STD-883H Test Method 1010.8 [35] or JEDEC Standard JESD22-A104D [32]. The standards state that for single chambers the dwell time has to be more than 10 min, whereas the transfer time should be less than 15 minutes. The test has to be conducted for at least 10 cycles. Teverovsky [36] suggested that the minimum number of cycles should be increased to 100 cycles in order to achieve a measurable effect on the reliability performance of tantalum capacitors. Since an increase of leakage current was observed, it was hypothesized that the local mechanical stresses, based on the coefficient of thermal expansion (CTE) mismatches, might have caused micro-cracking in the dielectric material, thus resulting in high current channels.

Accelerated tests are intended to precipitate the same failure mechanisms that occur under the normal operating conditions of the component. Due to the long operating life of tantalum capacitors, even at maximum rated stress conditions, accelerated testing is necessary to perform life testing within a reasonable timeframe so that the relevant failure modes and mechanisms can be identified. This can help in the development of part selection or qualification tests. The stress conditions for the accelerated tests have to be carefully chosen, since overstress conditions can result in failure mechanisms that may not be experienced in the usage conditions of the parts [38]. Electronic assemblies are often exposed to voltage stress and temperature cycling in their actual usage conditions. However, the failure modes and mechanisms relevant for the combined conditions have not yet been the subject of careful investigation. Accelerated testing, in the form of the Weibull grading test in MIL-STD-55365, involves constraining the acceleration factor to 20,000, which is equivalent to 1.5276 times the rated voltage at 85°C [29]. Higher voltage accelerations may be feasible for tantalum capacitors. Paulsen [33] hypothesized that testing of tantalum capacitors at highly accelerated electrical and thermal conditions at $3xV_R$ (rated voltage) and temperature up to 165°C did not reveal any new failure mechanisms. This was based on statistical analysis and was not confirmed by destructive failure analysis. Similar conclusions were made by Teverovsky [39], who conducted a highly accelerated life test (HALT) on solid tantalum capacitors with temperature stresses from 22°C to 130°C and voltage stresses from 1.25 x V_R to 2.25 x V_R. Virkki [40], [41] conducted a temperature cycling study on solid tantalum capacitors. Various tests were performed under temperature cycling conditions with and without applied voltage. A higher number of failures was observed in the experiment with added voltage compared to pure temperature cycling. The failure mechanism was not identified, but field crystallization was listed as a possible failure mechanism.

Previous studies have shown that the exposure of tantalum capacitors to simultaneous thermal and electrical stresses likely does not introduce unknown failure mechanisms. The studies also suggest that the acceleration factors of tests can be chosen to be higher than in current standards in order to reduce testing times. In this study, a new testing method is proposed in order to identify the dominant failure mechanisms and reduce testing times. In an accelerated test the parts were voltage step-stress tested in

steps from $1xV_R$ to $3xV_R$ during temperature cycling from -55 to +125°C. Instead of using 1 ampere to 2 ampere fuses, as suggested by MIL-PRF-55365H [29], failure criteria based on capacitance, dissipation factor, ESR, and leakage current specified by the manufacturers were used. Based on the literature, leakage current is expected to provide better sensitivity in detecting failures that are related to the degradation of the dielectric than fuses that trigger in the event of catastrophic failure. The samples were industrial grade 35 V tantalum capacitors from two different manufacturers with MnO_2 cathodes. The following sections describe possible failure mechanisms, the experimental approach, and the results. The last two sections report the findings of the failure analysis and the final conclusions.

2.2 EXPERIMENTAL WORK

2.2.1 APPROACH

Accelerated step-stress testing under temperature cycling was performed on solid tantalum capacitors with manganese dioxide (MnO_2) cathodes from two different manufacturers (referred to as manufacturer A and B) with EIA size code 2917. The electrical characteristics and dimensions for both capacitor designs were the same. A summary of the design parameters of the parts are shown in Table 1.
To avoid the pop-corning effect during the experiment, the residual moisture was removed from the capacitor packages by baking the parts for 24 hours at 125°C as proposed by JEDEC Standard JESD22-A113D. Electrical characterization of ten samples from each manufacturer was performed before and after reflow soldering, as well as in fixed intervals during the experiment. The measured electrical parameters were capacitance (C), equivalent series resistance (ESR), dissipation factor (DF), and leakage current (LC). All of the electrical parameters were measured in accordance with performance specification MIL-PRF-39003J at a temperature of 25°C, as shown in Table 8.

Electrical parameter	Voltage [V]	Frequency [Hz]	Electrification time [sec]
Capacitance	0.5 V_{rms}	120	-
Dissipation factor	0.5 V_{rms}	120	-
Equivalent series resistance	0.5 V_{rms}	100,000	-
Leakage current	35 V_{DC}	-	300

Table 8: Parameters of electrical characterization.

To eliminate the impact of the circuit resistance on the ESR measurements, a hand probing solution was used. Before the parts were exposed to temperature cycling, the effect of low temperatures and rated voltage stress for 72 hours was evaluated. In the next step the parts were cycled at temperatures from -55°C to +125°C while applying a voltage step-stress. Each voltage stress step was maintained for 72 hours, which was followed by electrical characterization. In the subsequent stress step the voltage stress was increased by one third of the rated voltage up to a maximum voltage stress of 3 x V_R. In order to not exceed the dielectric strength, the voltages were not increased after reaching the limit of 3 x V_R. To avoid power-on failures due to surge currents, the current was limited by 1 MΩ resistors in series. After each stress step, the parts were cooled down to 25°C, discharged, and electrically characterized. As degradation progressed, the failed samples were identified and extracted. The remaining capacitors were then exposed to the subsequent step-stress levels until failure occurred. Unstressed virgin samples and failed parts were used for failure analysis to identify the dominant failure mechanisms. Failure criteria were based on the MIL-PRF-55365 performance specification. Leakage current was measured after 5 minutes of electrification with rated DC voltage and should not exceed 2.4 µA. Capacitance and dissipation factor were measured at 120 Hz and 1 $V_{rms}$and should not exceed the capacitance tolerance of ±10 % and dissipation factor of 0.06 respectively. In addition, ESR was measured at 100 kHz and 1 V_{rms} and should not be higher than 1.3 Ω. A tabularized summary of the test plan is illustrated in Table 9.

Ratio of applied voltage/rated voltage [-]		1.00	1.00	1.33	1.66	2.00	2.33	2.66	3.00	3.00	3.00
Number of samples	Mfr. A	10	10	10	10	10	9	9	6	4	3
	Mfr. B	10	10	10	10	10	10	8	3	3	2
Temperature conditions		-55°C	Temperature cycling from -55°C to +125°C								

Table 9: Test conditions for 10 parts from each manufacturer.

2.2.2 Results of Step-Stress Testing and Temperature Cycling of Tantalum Capacitors

The following figures show the measurements of capacitance, dissipation factor, ESR, and leakage current over the duration of the experiment obtained in 72-hour intervals. Leakage current proved to be the most accurate indicator of tantalum capacitor degradation. At the termination of the experiment, 7 of 10 capacitors and 8 of 10 capacitors failed from manufacturer A and manufacturer B, respectively.
Figure 22 and Figure 23 depict the leakage current degradation trend for manufacturer A and manufacturer B samples. Since degradation of electrical parameters was observable in leakage current, we believe that the temperature and voltage stresses mainly affected the dielectric layers. This behavior is in agreement with the discussion of dominant failure modes and mechanisms in section **Error! Reference source not found.**. The initial stress step at rated voltage of 35V and a constant temperature of -55°C resulted in no noticeable degradation for parts from manufacturer A, and only slight degradation for parts from manufacturer B. The degradation trends of both populations show a similar pattern, with no early failures. The concern that the voltage levels were in the overstress domain can be rejected, since no abrupt increases of leakage current were observed. Instead, the parts experienced a slow increase of leakage current, suggesting an incremental degradation of the dielectric.

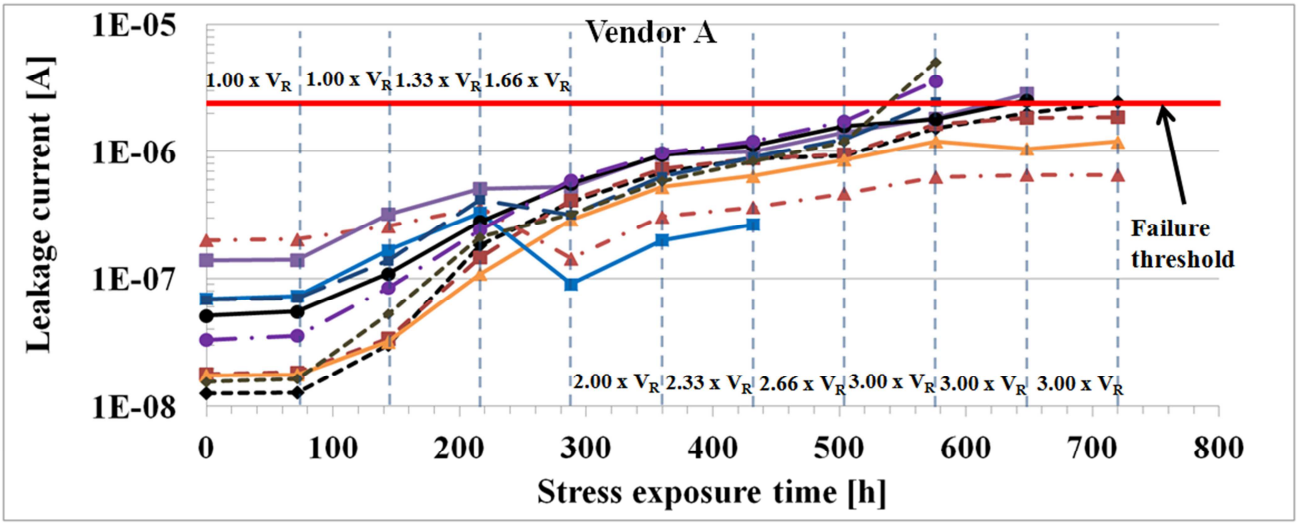

Figure 22: Degradation of leakage current in 10 samples from manufacturer A during voltage step-stress testing while temperature cycling from -55°C +125°C.

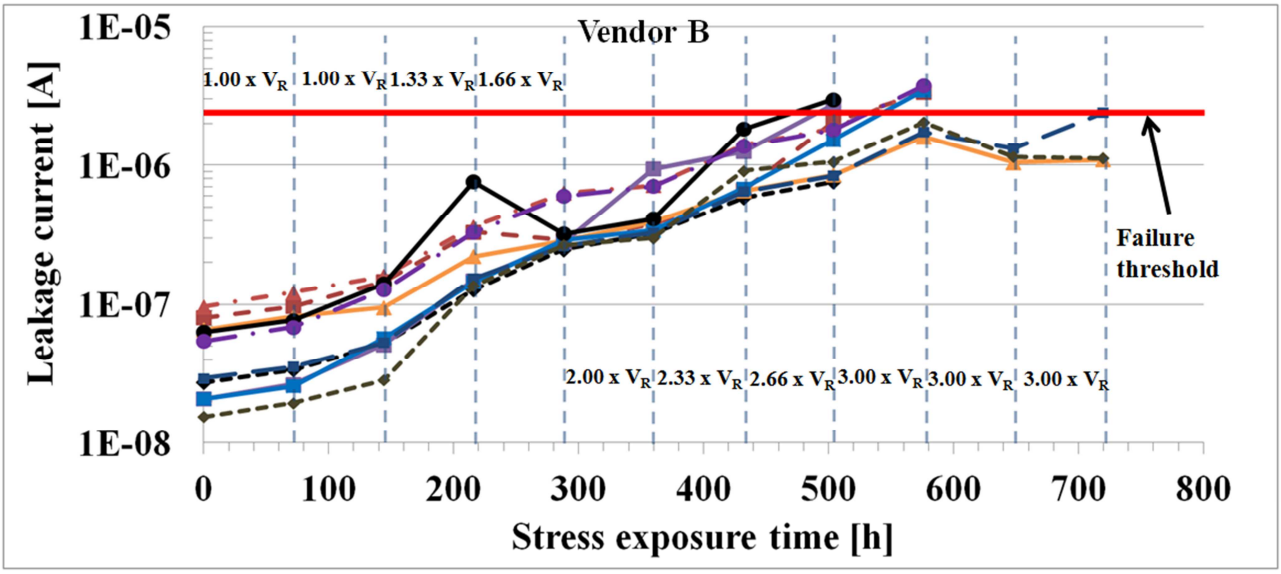

Figure 23: Degradation of leakage current in 10 samples from manufacturer B during voltage step-stress testing while temperature cycling from -55°C to +125°C.

Thermo-mechanical and electrical stresses were not expected activate a wearout mechanism that resulted in changes in the dielectric thickness, dielectric constant or effective electrode area. Degradation of capacitance was either not or only marginally measurable in both populations. Samples from manufacturer A showed a stabilized capacitance over the entire test duration, whereas samples from manufacturer B showed an overall capacitance decrease of about 2–3%. A decrease in capacitance in the population can be explained by residual moisture in the porous tantalum pellet, which was trapped between the dielectric and cathode layer and effectively increased the electrode area, thus increasing the capacitance of the parts. Moisture desorption during the high temperature dwells could have reduced the effective electrode surface in manufacturer B parts as observed by Teverovsky [42].

ESR is governed by dielectric losses due to the purely resistive component of a capacitor. This resistance is composed of the bulk resistivities of the materials, contact resistances between the layers, and termination resistances. Increase of ESR in tantalum capacitors is often related to high thermo-mechanical stresses resulting from quick temperature changes as experienced in processes such as reflow soldering and CTE mismatches. The thermo-mechanical stresses could cause detachment of the cathode from the dielectric which is attached with silver adhesive. The reduced contact area will then result in an increase of ESR. Similarly, as observed by Teverovsky [36], measurements of equivalent series resistance (ESR) showed no significant degradation in our experiment. No increase of ESR during the experiment, as well as after reflow soldering, was noticeable. The values of ESR after reflowing were well below the failure threshold, which was not reached during the experiment. This suggests that even temperature cycling at the extremes of the maximum specified temperatures, ranging from -55°C to +125°C, are not a critical condition for attachment of the lead frames to the tantalum pellets. We observed a high variation of ESR, which resulted in unstable trends of ESR. This is due to the manual probing, which does not allow control of the contact area between the capacitors and the probe. In future experiments this will be replaced by a permanent soldered connection instead.

Dissipation factor degradation was insignificant for both manufacturer populations. A slightly higher variation of dissipation factor among the population of manufacturer B was noticeable compared to parts from manufacturer A. Since dissipation factor is proportional to ESR (Equation 7), degradation of dissipation factor were not observed except for one case. While all samples failed due to an increase of leakage current, only one sample showed an additional increase of dissipation factor from 0.0075 to 0.155. Even though leakage current and dissipation factor are not directly related, we believe that the

breakdown of the dielectric had an effect on both parameters in this sample. Since the dissipation factor is the sum of the DC conductivity and relaxation losses in the dielectric [43], [44], we believe that the breakdown in this sample could have had an effect on the conductivity of a large volume within the bulk material. However, structural changes were not observed in failure analysis of the sample to support this hypothesis.

$$\boldsymbol{DF = \frac{ESR}{X_C}} \quad \textbf{(7)}$$

2.3 Failure Analysis

The previous analysis shows that degradation was primarily observed as an increase in leakage current. This indicates that the dielectric layers were predominantly affected by the selected electrical and thermal stresses. Various failure mechanisms, such as field crystallization, micro-cracking, or oxygen migration, could be responsible for the degradation of the dielectric. Cross-sectional analysis was performed to identify whether the thermo-mechanical stresses resulting from temperature cycling had any effect on the delamination of the lead frame attachment from the tantalum pellet. While no delamination or detachment of the lead frames was observed, some cross-sectioned samples from manufacturer A showed cracking of the silver adhesive (Figure 24). However, since the contact area between the lead frame and the tantalum pellet provided by the silver adhesive was large compared to the crack, no measurable effect of cracking on ESR was observed.

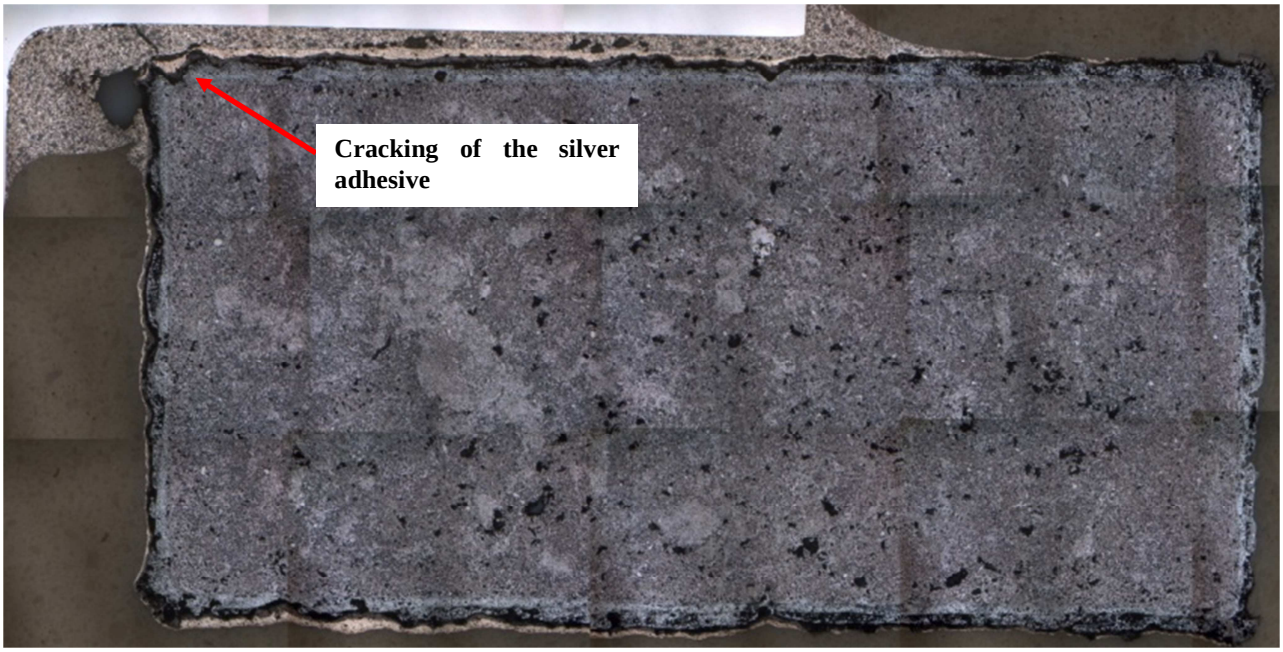

Figure 24: Cross-section of failed sample from manufacturer A showing cracking of the silver adhesive. The image was acquired using bright-field optical microscopy.

Since dielectric breakdown occurs on a small scale, discovery of dielectric breakdown sites can be challenging. The tantalum pellet is a porous structure and, as such, the breakdown sites can be located anywhere within the pellet's body. Since degradation of leakage current was observed, a suitable method for the examination of a large dielectric surface was required. Decapsulation of the tantalum pellet was chosen due to its exposure of the tantalum pellet without removal of the dielectric. The application of various acids at elevated temperatures removed the mold compound, the lead frames, and the contacting layers (Ag, C, MnO_2). Decapsulated unstressed samples from both manufacturers are shown in Figure 25 and Figure 26.

This technique exposes the external dielectric surface but does not allow identification of the dielectric breakdown that occurred within the tantalum pellet. Electroplating can be used to assess the degradation of the dielectric on the exposed surfaces of the tantalum pellet. Decapsulated virgin and failed samples were electroplated with tin at a voltage of 0.3 V for 15 minutes. The level of degradation in the dielectric can be assessed by the amount and magnitude of tin-plated spots that mark the high current channels. While virgin samples showed only a few small tin-plated areas, failed samples showed numerous larger tin-plated areas for parts from manufacturer A () and manufacturer B (). This observation suggests that stresses were concentrated in these areas and caused locally restricted degradation of the dielectric rather than homogeneous degradation.

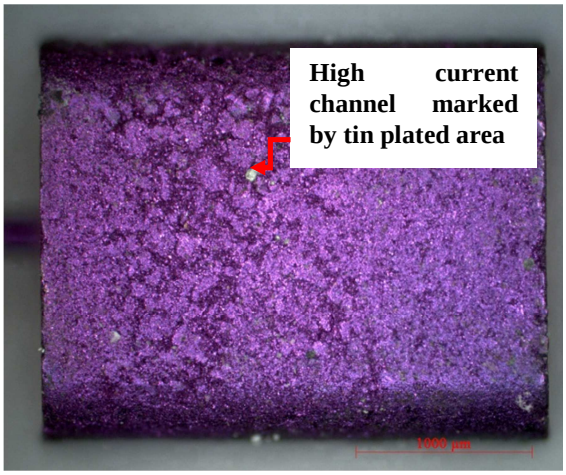

Figure 25: Decapsulated virgin capacitor from manufacturer A after tin plating under reverse voltage.

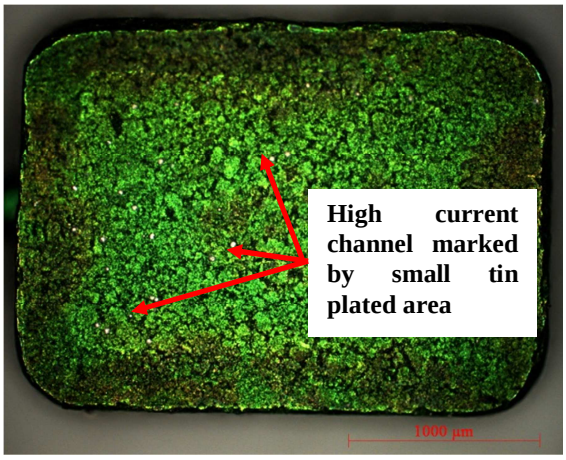

Figure 26: Decapsulated virgin capacitor from manufacturer B after tin-plating under reverse voltage.

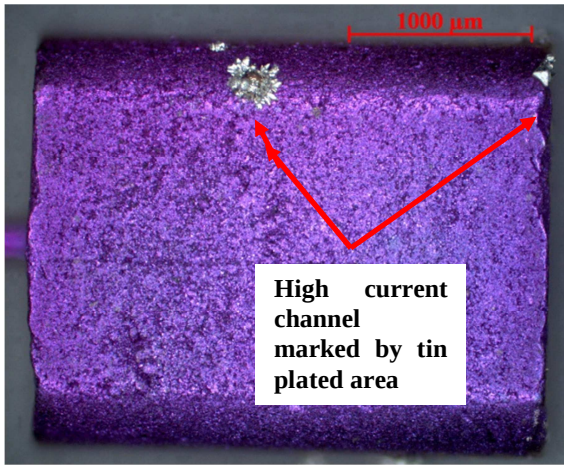

Figure 27: Decapsulated step-stress tested capacitor from manufacturer A after tin plating under reverse voltage.

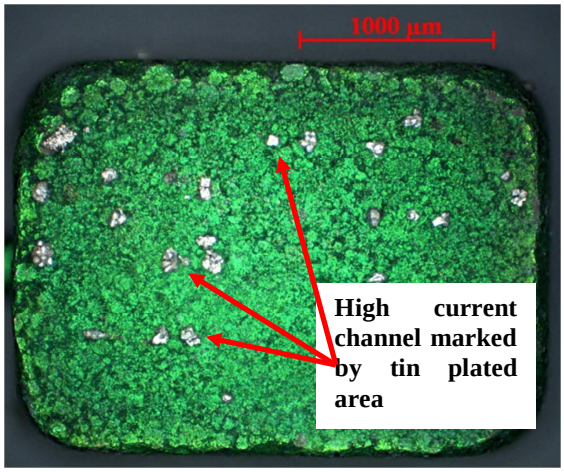

Figure 28: Decapsulated step-stress tested capacitor from manufacturer B after tin plating under reverse voltage.

The color differences of the pellet surfaces are noticeable. We observed that all samples from manufacturer A showed a purple-colored dielectric surface, whereas the dielectric of manufacturer B parts was green-colored. The color discrepancies can be explained by the constructive and destructive interference of light reflecting from the front and back surface of the dielectric. The color depends on the thickness, which is closely related to the forming voltage, of the light-transmissive dielectric, thus allowing us to make a qualitative comparison between the two capacitor designs. The green-colored dielectric of manufacturer B indicates a thicker dielectric as compared the purple-colored dielectric from manufacturer A [13]. To quantify the dielectric thicknesses of parts from both manufacturers, cross-sections of virgin and failed parts were analyzed using an environmental scanning electron microscope (ESEM). The measurements of dielectric thicknesses were obtained in the vicinity of the center of the tantalum pellet (Table 10) as well as in the peripheral region of the pellet (Table 11).

	Manufacturer A		**Manufacturer B**	
	Virgin parts	**Failed parts**	**Virgin parts**	**Failed parts**
Avg. [nm]	**262**	**258**	**226**	**220**
Std. [nm]	**18**	**15**	**18**	**17**
Sample size	**44**	**45**	**45**	**44**

Table 10: Summary of measurements of dielectric thicknesses in the vicinity of the center of the tantalum pellet.

	Manufacturer A		**Manufacturer B**	
	Virgin parts	**Failed parts**	**Virgin parts**	**Failed parts**
Avg. [nm]	**306**	**302**	**351**	**331**
Std. [nm]	**28**	**21**	**25**	**37**
Sample size	**45**	**44**	**39**	**45**

Table 11: Summary of measurements of dielectric thicknesses in the vicinity of the peripheral region of the tantalum pellet.

Comparing the results of the measurements in the vicinity of the outer surface from both manufacturers, we confirmed that the dielectric thicknesses of parts from manufacturer B were higher than in parts from manufacturer A on the external surfaces (Table 10). Interestingly, we observe the opposite in the center region of the pellet, where parts from manufacturer A have a higher thickness (Table 11). It is likely that the lower dielectric strength observed in the center of the pellets is related to the actual robustness of the parts. The reduced dielectric thickness found in areas close to the center of the parts can be explained by the lesser degree of penetration by the solution used for the dielectric formation process into the center of the tantalum pellet. Other factors affecting the dielectric thickness in the center could be the amount of pressure when forming the tantalum pellet or the shape of the tantalum particles. The tantalum particles of manufacturer A are string-shaped, whereas manufacturer B uses spherically shaped particles that allow closer packing. A comparison of the dielectric thicknesses of virgin and failed parts did not reveal significant differences in dielectric thickness. This was also observed on decapsulated samples, where a color change of the dielectric between virgin and failed parts was not noticeable.

The decapsulated sample surfaces of virgin and failed parts were inspected at high magnifications using an environmental scanning electron microscope (ESEM). Occurrences of micro-cracking that might have been responsible for the increased leakage current were not observed on the surfaces. Field crystallization was observed on all samples. Virgin parts showed field crystallization sites in small

numbers distributed over a large area (Figure 29). Failed samples showed a large number of crystallization sites restricted to a small area (Figure 30), which suggests that the leakage current increase is also restricted to small areas instead of being distributed uniformly within the bulk of the tantalum pellet. This aligns with the observations made after the tin-plating of the decapsulated failed samples. The temperature stress could have also caused oxygen migration as an additional failure mechanism. Unfortunately, electron dispersive spectroscopy (EDS) did not allow elemental analysis on a small scale as the interface of the tantalum metal and the dielectric, where oxygen migration could occur. Therefore, the impact of oxygen migration on the degradation of the samples could not be identified.

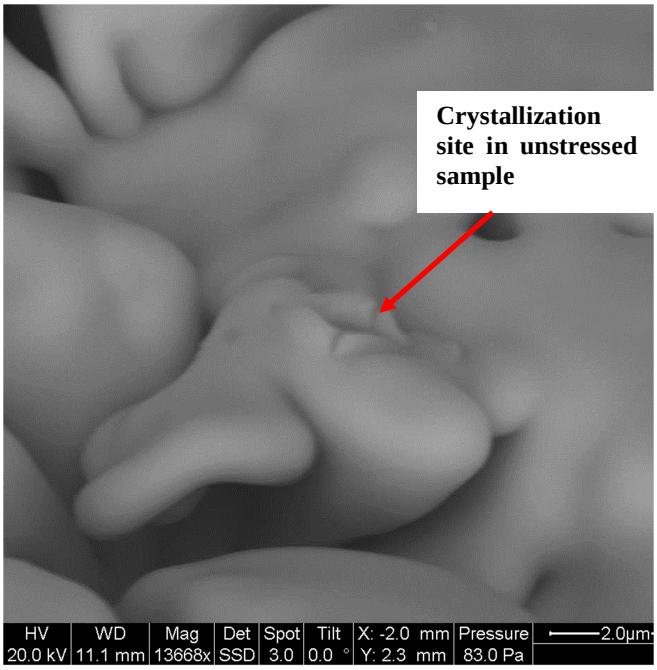

Figure 29: Crystallization site observed on virgin sample from manufacturer A.

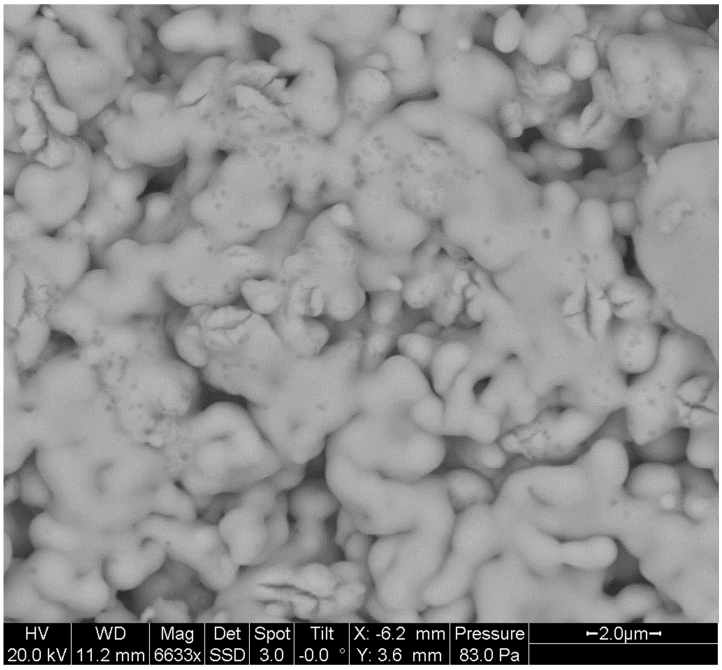

Figure 30: Numerous crystallization sites restricted to small area on failed sample from manufacturer B.

2.4 SUMMARY AND CONCLUSIONS

Tantalum capacitors with manganese dioxide cathodes often experience concurrent temperature and voltage stresses in their actual usage conditions, which have both been identified to be critical for tantalum capacitor degradation. The relevant failure modes and mechanisms due to simultaneous exposure to voltage and temperature cycling stresses have not previously been the subject of a systematic study. The robustness of two competing tantalum capacitor designs to voltages up to 3 x V_R while temperature cycling between -55°C to +125°C was assessed. Both populations showed a similar number of failures with 7 of 10 samples of manufacturer A and 8 of 10 samples from manufacturer B. Leakage current was the most sensitive parameter related to the degradation of the parts, while the other parameters did not indicate degradation. Thus, a failure criterion based on leakage current should be used in life testing of tantalum capacitors.

Failure analysis confirmed that the stress conditions affected the dielectric layer. The observed failure mechanisms were consistent with the failure mechanisms that were identified in previous studies at lower stress levels, which confirmed that the highly accelerated stress conditions did not introduce new failure mechanisms. Increased densities of field crystallization sites were observed on the dielectric surfaces of failed samples. While micro-cracking due to thermo-mechanical stresses was not observed, oxygen migration cannot be rejected as another possible failure mechanism. Inspection of decapsulated samples indicated higher dielectric thicknesses of parts from manufacturer B. However, analysis of the dielectric thicknesses revealed a dielectric thickness gradient between external surfaces and the center of the tantalum pellets. In the center of the tantalum pellets, parts from manufacturer A had higher dielectric thicknesses than parts from manufacturer B, which might result in a lower life performance of manufacturer B parts, but degradation of the parts depended on other factors such as impurities and

oxygen distribution within the dielectric material, as well. The dielectric thickness gradient also suggests that failure sites may be concentrated at the center of the pellets, where dielectric thicknesses are significantly lower than in the peripheral regions.

Temperature cycling and voltage stress are usually inevitable conditions under which tantalum capacitors operate in their applications. Since both types of stresses are critical for the degradation of the thermodynamically unstable dielectric, a thorough understanding of the effects of these stresses on the reliability of solid tantalum capacitors is necessary to develop qualification and screening tests that address reliability risks experienced in the field. The results have shown that the highly accelerated stress conditions in this test did not lead to new or unknown failure mechanisms. We showed that voltage stress acceleration can be as high as three times the rated voltage, depending on the capacitor type. This can lead to shorter qualification or screening test times as compared to the standard qualification test time of 2000 h of the Weibull grading test. Further, the effects of thermo-mechanical stresses due to temperature cycling in this experiment remained insignificant, suggesting that a larger range of temperatures might be appropriate for qualification tests designed for high temperature applications that address reliability risks in temperature cycling conditions.

2.5 RECOMMENDED FUTURE WORK

The motivation of this study was not to obtain exhaustive data for statistical analysis, which led to limited sample size in this experiment. In addition to confirming with failure analysis in this study that the step-stress testing method, compared to constant stress testing, does not introduce any other failure mechanism, it could be beneficial to conduct a constant stress reliability study with a larger sample sizes to allow statistical comparison of this approach to traditional methods of life testing.

2.6 CONTRIBUTIONS

The study described in the thesis examined the effect of simultaneous thermo-mechanical and electrical stresses on tantalum capacitors with manganese dioxide cathodes. The objective was to identify the dominant failure mechanism due to these stress conditions.
The contributions were as follows:

- Identified the dominant failure mechanism of simultaneous exposure to temperature cycling and voltage stress. Field crystallization was identified as the primary failure mechanism.
- Identified that the dielectric thickness on the tantalum pellet surface is not a reliable indicator of quality control. Significant differences of the dielectric thickness between the center and peripheral area of the tantalum pellet were observed. This suggests that the consideration of the dielectric thickness in the center of the tantalum pellet has to be considered as a potential failure site in weak populations.

3 REFERENCES

[1] E. Reed, “Characterization of Tantalum Polymer Capacitors.” NASA NEPP Task 1.21.5, Phase 1, FY05, URL: http://nepp.nasa.gov/docuploads/0EA22600-8AEC-4F47-9FE49BAABEAB569C/Tantalum Polymer Capacitors FY05 Final Report.pdf [Accessed: 12/6/12].

[2] D. Tian, H. Wang, and Q. Pan, “The Performances Contrastive Analysis of Chip Tantalum Capacitor and MLCC,” in CARTS International 2012 Symposium Proceedings, Las Vegas, Nevada, 2012, pp. 1–11.

[3] J. D. Prymak and M. Prevallet, “Scintillation Testing of Solid Electrolytic Capacitors,” in Proceedings of 26th Symposium for Passive Components, Orlando, Florida, 2006, pp. 395–406.

[4] A. Teverovsky, “Scintillation and Surge Current Breakdown Voltages in Solid Tantalum Capacitors,” IEEE Transactions on Dielectrics and Electrical Insulation, vol. 16, pp. 1134–1142, 2009.

[5] A. Teverovsky, “Scintillation Breakdowns and Reliability of Solid Tantalum Capacitors,” IEEE Transactions on Device and Materials Reliability, vol. 9, no. 2, pp. 318–324, Jun. 2009.

[6] J. Gill, “Surge in Solid Tantalum Capacitors.” AVX Ltd.

[7] R. W. Franklin, “Surge Current Testing of Resin Dipped Tantalum Capacitors.” AVX Ltd., 1985.

[8] B. Long, M. Prevallet, and J. D. Prymak, “Reliability Effects with Proofing of Tantalum Capacitors,” in Proceedings of 25th Symposium for Passive Components Conference, Huntsville, AL, 2005, pp. 167–171.

[9] J. D. Prymak, M. Prevallet, and P. Staubli, “Proofing Tantalum Capacitors and Effects on Reliability,” in CARTS Europe 2005 Symposium Proceedings, Prague, Czech Republic, 2005, pp. 171–178.

[10] E. Chan, J. D. Prymak, and D. Wang, “Power-On Failures in Tantalum and Aluminum SMT Capacitors,” in Proceedings of the 5th Conference on Electronic Materials and Packaging, Singapore, 2003.

[11] KEMET Electronics Corp., “Tantalum Surface Mount Capacitors – Standard Tantalum,” pp. 3–5, Jan. 2011.

[12] VISHAY Intertechnology, Inc., “Solid Tantalum Surface Mount Chip Capacitors, Molded Case, Standard Industrial Grade Catalogue.” VISHAY Intertechnology, Inc., 30-Aug-2012.

[13] J. Gill, “Basic Tantalum Capacitor Technology,” AVX Corp., pp. 1–7, Jul. 1994.

[14] B. Goudswaard and F. J. J. Driesens, “Failure Mechanism of Solid Tantalum Capacitor,” Electrocomponent Science and Technology, vol. 3, no. 3, pp. 171–179, 1976.

[15] Y. Freeman, R. Hahn, and J. Prymak, “Reliability and Critical Applications of Tantalum Capacitors,” in CARTS Europe 2007 Symposium Proceedings, Barcelona, Spain, 2007, pp. 111–121.

[16] T. Zednicek, J. Sikula, and L. Leibovitz, “A Study of Field Crystallization in Tantalum Capacitors and its Effect on DCL and Reliability,” in CARTS USA 2009 Symposium Proceedings, Jacksonville, Florida, 2009, pp. 1–16.

[17] J. Hossick-Schott, “A Charge Based Model for Time Progression of Field Crystallization in Tantalum Pentoxide,” in CARTS USA 2009 Symposium Proceedings, Jacksonville, Florida, 2009, pp. 1–8.

[18] J. Sikula, V. Sedlakova, H. Navarova, and J. Majzner, “Leakage Current and Noise Reliability Indicators for Ta and NbO Low Voltage Capacitors,” in CARTS USA 2010 Symposium Proceedings, New Orleans, Louisiana, 2010, pp. 1–13.

[19] J.-P. Manceau, S. Bruyerel, S. Jeannot, A. Sylvestre, and P. Gonon, “Leakage Current Variation With Time in Ta2O5,” in IEEE International Integrated Reliability Workshop Final Report 2006, Lake Tahoe, California, 2006, pp. 129–133.

[20] L. L. Odynets, “Field Crystallization Model in Metal-Oxide-Electrolyte Systems,” Soviet Electrochemistry, vol. 23, no. 12, pp. 1591–1594, Dec. 1987.
[21] D. A. Vermilyea, “The Crystallization of Anodic Tantalum Oxide Films in the Presence of a Strong Electric Field,” Journal of the Electrochemical Society, vol. 102, no. 5, pp. 207–214, May 1955.
[22] J. D. Prymak, “Replacing MnO2 with Conductive Polymer in Tantalum Capacitors,” in CARTS USA 1999 Symposium Proceedings, New Orleans, Louisiana, 1999, pp. 1–6.
[23] J. Marshall and J. Prymak, “Surge Step Stress Testing (SSST) of Tantalum Capacitors,” in CARTS 2001 Symposium Proceedings, 2001, pp. 1–7.
[24] A. Teverovsky, “Reliability Effects of Surge Current Testing of Solid Tantalum Capacitors.” NASA, Dec-2007.
[25] B. M. Mogilevsky and G. A. Shirn, “Surge Current Failure in Solid Electrolyte Tantalum Capacitors,” IEEE Transactions on Components, Hybrids,and Manufacturing Technology, vol. 9, no. 4, pp. 475–479, Dec. 1986.
[26] E. K. Reed, “Tantalum Chip Capacitor Reliability in High Surge and Ripple Current Applications,” in Proceedings of 44th Electronic Components and Technology Conference, Washington D.C., 1994, pp. 861–868.
[27] H. W. Holland, “Effect of High Current Transients on Solid Tantalum Capacitors.” KEMET Electronics Corp., 1996.
[28] A. Teverovsky, “Effect of Surge Current Testing on Reliability of Solid Tantalum Capacitors,” in Proceedings of 28th Symposium for Passive Components Conference, Newport Beach, CA, 2008, p. 293.
[29] Department of Defense, “Performance Specification - MIL-PRF-55365H.” Department of Defense, MIL-PRF-55365H, Section 4.7.20, pp. 29-31, Feb-2011.
[30] A. Teverovsky, “Effect of Inductance and Requirements of Surge Current Testing of Tantalum Capacitors,” in CARTS 2006 Symposium Proceedings, 2006, pp. 234–256.
[31] A. Teverovsky, “Scintillation Breakdowns in Chip Tantalum Capacitors,” in Proceedings of International Microelectronics and Packaging Society, Brno, Czech, 2008, pp. XL–LII.
[32] JEDEC Standard JESD22-A113D, “Preconditioning of Nonhermetic Surface Mount Devices Prior to Reliability Testing.” JEDEC Solid State Technology Association, Aug-2003.
[33] J.-L. Paulsen, “Reliability Characterization of Tantalum Capacitors with MnO2 Counter-Electrode,” in CARTS Europe 2006 Symposium Proceedings, Bad Homburg, Germany, 2006, pp. 1–12.
[34] AVX Corp., “AVX Tantalum and Niobium Oxide Capacitors – TAP/TEP Technical Summary and Application Guidelines,” Volume 11.8, pp. 131–139.
[35] Department of Defense, “Temperature Cycling - MIL-STD-883H.” Department of Defense, Method 1010.8, Jun-2004.
[36] A. Teverovsky, “Effect of Temperature Cycling and Exposure to Extreme Temperatures on Reliability of Solid Tantalum Capacitors,” NASA Electronic Parts and Packaging, pp. 5–17, Jan. 2007.
[37] KEMET Electronics Corp., “Surface Mount Capacitors.” 01-Apr-2010.
[38] H. Pham and E. Elsayed, Handbook of Reliability Engineering, 1st ed. Springer, 2003.
[39] A. Teverovsky, “Analysis of Weibull Grading Test for Solid Tantalum Capacitors,” in CARTS Europe 2010 Symposium Proceedings, Munich, Germany, 2010, pp. 1–18.
[40] J. Virkki and P. Raumonen, “Testing the Effects of Seacoast Atmosphere on Tantalum Capacitors,” Active and Passive Electronic Components, vol. 2011, no. 108423, pp. 1–9, 2011.
[41] J. Virkki and S. Tuukkanen, “Testing the Effects of Temperature Cycling on Tantalum Capacitors,” Microelectronics Reliability, vol. 50, no. 8, pp. 1121–1124, Aug. 2010.

[42] A. Teverovsky, “Effect of Moisture on Characteristics of Surface Mount Solid Tantalum Capacitors,” in Proceedings of the 23rd Capacitor and Resistor Technology Symposium, Scottsdale, AZ, 2003, pp. 96–111.
[43] P. Lunkenheimer, S. Krohns, R. Fichtl, S. G. Ebbinghaus, A. Reller, and A. Loidl, “Colossal Dielectric Constants in Transition-Metal Oxides,” Eur. Phys. J. Special Topics, vol. 180, pp. 61–89, Dec. 2009.
[44] S. Vangchangyia, E. Swatsitang, P. Thongbai, S. Pinitsoontorn, T. Yamwong, S. Maensiri, V. Amornkitbamrung, and P. Chindaprasirt, “Very Low Loss Tangent and High Dielectric Permittivity in Pure-CaCu3Ti4O12 Ceramics Prepared by a Modified Sol-Gel Process,” J. Am. Ceram. Soc., vol. 95, no. 5, pp. 1497–1500, 2012.